Topic Editor Decision: Reconsider after major revisions (21 Sep 2020) by John M. Huthnance
Comments to the Author:

Dear Authors
Thank-you again for your revised manuscript. I am sorry for the delay in obtaining reviews and getting them on the Editorial system. Both reviews raise serious comments of presentation and there are a few serious aspects of science also for you to address – statistics of results, Ekman transports. I am copying these comments below for your convenience (plus a couple of mine at the end). These comments will be public if or when your manuscript is published, so readers will be able to see whether you have answered them satisfactorily. I may want to send it back to the reviewers again. Please also be sure that your text is clear (Reviewer 4 makes many points). A final manuscript will be copy-edited, but the copy-editor cannot be expected to guess what you mean.
Yours sincerely
John Huthnance (editor)

Reviewer 1

Second review of Tarasenko et al., Surface waters properties in the Laptev and the East-Siberian Seas in summer 2018 from in situ and satellite data, submitted to Ocean Science.

In this second review, I refer back to my first review, and to the authors' responses to that review.

In the Overview, I noted that the Introduction section and the Discussion and Conclusions section needed to be improved.

The Introduction is now much better, but there is still an important missing point. The Arctic stores, imports and exports huge volumes of freshwater (as the authors note), but when concentrating on the shallow Siberian shelf seas, they make no comment about their role as conduits for freshwater. Their importance is more that the large river runoff volumes must cross the shelf seas before they reach the Beaufort Gyre / Canadian Basin (and find their eventual fate through export out of the Arctic). How do these freshwaters cross the shelf seas to the deep basins? Our understanding of processes / dynamics / timescales is incomplete, and this is where Armitage (2016) is helpful - it is not just about the small downwards storage trend in the shelf seas, it is also about comparisons of storage variability between deep and shallow basis.

The authors should also consider Schlosser et al. (DSR I, 1994) "Arctic river runoff: mean residence times on the shelf and in the halocline". Has this excellent work been updated? In any event, they show from geochemical measurements that river waters spend two or three years in the shelf seas before leaving offshore. How does this fundamental observation reflect on the authors' findings?

Answer:

Thank you for your suggestions. We modified the Introduction adding the citation of Schloesser et al. (1994) and a more recent study of geotracers in the Arctic (2020), published after we sent our paper to OS in May 2019.

As for the storage variability between deep and shallow basins, I would like to leave this subject for a different study, as it does not concern the small-scale variability presented in this paper. A theory that the Beaufort gyre accumulates most of the fresh water entering the Arctic over the shelf needs to be confirmed for the period after 2014 (so after the study of Armitage 2016), as the sea ice regime has changed significantly over last 6 years.

Nevertheless, the reviewer's comment made us think that we should have put more emphasis in the introduction on the interest of satellite sea surface salinity for monitoring the fate of the freshwater on the shelf, so we have added:

The salinity provides precious information about the fate of the freshwater river input. In this paper, we look at the information accessible with satellite salinity. While this information is restricted to the top sea surface, the regular and synoptic monitoring of sea surface salinity from space allows to document its spatio-temporal variability in great details not accessible with any other means, providing a new tool for analyzing some of the processes at play.

Regarding the Discussion and Conclusions - I am mainly happy with the revised text but see my point 10 below for a specific (continuing) problem.

I next consider the authors' replies to my specific points.
1, 2, 3, 4, 5. OK, thanks.

6. You state in section 2.2.3 (line 19 in v5) that the SMOS spatial resolution is about 50 km, so that oversampling at 15 km means that each 50 x 50 km2 resolved area contains about ten 15 x 15 km2 points, and oversampling means that those ten points will contain noise around the "true" mean of the 50 km grid cell. So I repeat my question: how does this affect your statistics?
Answer:
This is not what we meant. SMOS SSS are representative of SSS integrated over about 50x50km2 given the footprint of SMOS radiometric measurements involved in the SSS retrievals. The SMOS radiometric measurements are integrated over approximately a 50km x 50km area. We don't make any spatial average. The oversampling on a 15km grid is possible owing to the image reconstruction of the SMOS interferometric data, but in our processing we don't make any spatial average.

7. OK, thanks.

8. OK, I am happy with your explanation but you need to note in the relevant figure captions that the virtual transects are shown by the red lines.
Answer:
Corrected, thank you

9. OK, thanks.

10. No problems with Ekman transport, but the Ekman pumping calculation in shallow water is simply not valid. Just because you can solve an equation does not mean that use of the equation is valid. If this is at all unfamiliar, I recommend the nice online textbook by Robert Stewart of Texas A&M (search for "Stewart oceanography text book", it is available for free download) and look at the Ekman sections (in chapters 9, 12). The balance of operative processes is very different in shallow (tens or a few hundreds of metres) versus deep (thousands of metres) waters, which is why I suggested looking at the Lentz papers (JFM 2002, JPO 2004, and Moffat & Lentz, JPO 2012). I also recommend Whitney & Garvine (JGR 2005) as a nice illustration / application of the framework. They describe upwelling and downwelling response to winds and Ekman transports in shallow waters (including buoyant coastal currents). This would provide a credible framework to describe your observations, and not Ekman pumping. You do not necessarily need to do more analytical work, that is not what I am asking for. But you need to remove the Ekman pumping results from your figures, and then interpret the Ekman transports in shallow-water terms.

For example, in your v5 figure 15 panel c, showing an east wind with offshore Ekman transport, that will induce downwelling at the coast and a consequent residual vertical circulation that draws water from offshore onto the shelf below the surface layer. Same figure panel f shows a south wind that induces a mainly along-shore Ekman transport that probably does not induce a residual vertical circulation. This style of interpretation would improve the Discussion and Conclusions.

Answer:
Corrected, please see a new version of "Discussion and Conclusion"

11. This is an additional point. The manuscript should become publishable subject to the remaining problems being fixed, but the presentation of text in figures (mainly axis and contour labels) is poor. Text is often much too small for sensible legibility. Please check each figure, consider what size the text might appear on the printed page, and make it all a readable size.
Answer: Thank you, we tried to correct it

Reviewer 4

Summary
In this paper, the authors use a combination of satellite and in-situ data to document the evolution of water masses in the Laptev and East Siberian Sea of the summer of 2018. The focus is on the surface layer, and in particular, water masses deriving from the Lena River and low salinity waters from the Kara Sea.

The authors make use of CTD transects undertaken in the ARKTIKA-2018 expedition to evaluate the accuracy of satellite SST and SSS products. For the latter, the authors themselves present a novel SSS product that they deem to be most appropriate for the geographical region under question. The authors argue that the match between the satellite products and the in situ data is sufficiently strong that the satellite products themselves can be used for much of the remaining analysis in the paper, in particular, defining separate water masses and tracing their evolution over the late summer 2018 period.

Using a TS framework to separate the water masses, the authors resolve spatial changes in the water masses over time. They also focus attention onto particular sections in order to make links between water mass changes and other processes: wind speed and the passing of cyclones. The authors present geochemical analysis from the cruise transects that helps to verify the origins of the surface water masses between the tree end members: river water, sea ice melt, and marine water.

This paper is a useful documentation of the surface ocean in the Laptev and East Siberian Sea in the summer of 2018, and to that extent that the authors successfully make process-based findings, it has implications beyond the time frame during which the measurements were made. The methods are mostly appropriate for the chosen questions, though I have some specific suggestions in terms of robustness of the evaluation of satellite data, and the means of comparison of certain physical data.

Novel oceanographic data and novel SSS satellite retrievals are presented, but it is not quite true that the presentation of water mass properties at a synoptic scale in this region of the Arctic is totally novel (see Osadchiev et al., 2020, Scientific Reports).

The paper of Osadchiev et al. 2020 was submitted in March 2020 so later than the initial submission of our paper that was available for public review and discussion on 31 July 2019 on Ocean Science Discussion.

The significance of the work is largely in its implications for the usefulness of satellite SST and SSS in the Arctic, though in my view the authors have more work to do on that point. The communication of the results and methods needs some improvement, both in text and figures.

Main points
Evaluation of satellite data.

The authors present co-located surface water (CTD and TSG) measurements and satellite data in scatter plots. The authors also provide a useful error frequency distribution, from which they show that the observed errors are more substantial than that provided by the satellite product (for both SST and SSS). After discussing the comparison to in situ data, the authors simply resolve that the two products agree well with the in situ data and use this as support for using the products for the following analyses. A more robust justification is required, especially given that the differences to the in situ data are not insignificant.

Can the authors use existing conventions in the literature for what constitutes a "good agreement"?
Another approach would be to think about how sensitive the key findings are to random error and biases in the satellite data. Can the authors comment on what threshold of random error or bias the data must be below in order for the results to be robust?

If it can be demonstrated that the results are not sensitive to the present level of error in the measurements, that would be more convincing evidence to the reader that the data are appropriate to be used.

Answer:
We think that part of the reviewer's remark comes from an abuse of language. What was called 'error on DMI estimated SST', 'theoretical error' on SMOS SSS (following the terminology employed in the SMOS measurements documentation) or 'error on SMOS ESA L2 SSS' is in fact an uncertainty; for instance in the case of SMOS, it corresponds to the expected standard deviation between the true SSS value and the SMOS SSS as derived by the SMOS retrieval scheme based on uncertainties on the SMOS brightness temperatures and ancillary measurements used in the retrieval. Hence what is shown on Figure 4d, or 5d is that the statistical distribution of the differences between satellite-in situ SSS is in rather good agreement with the uncertainties of the satellite measurements. However, it is not possible to thoroughly validate these uncertainties in this paper as it would require much more measurements: actually, as shown on Figure 4b and 5b the uncertainties vary much over the area so that a validation of the uncertainty would require large number of measurements for each class of uncertainty value. We have made the vocabulary clearer and we now explain how Fig 4d and Fig 5d show that the order of magnitude of the observed errors is in agreement with the product uncertainties and that these errors are much smaller than the observed spatial gradients shown on Fig 4a and 5a.

Surface water-mass TS analysis

It is inevitable that the separation of water masses into distinct groups will be based on somewhat arbitrary salinity and temperature values. However, the authors need to do a bit more to explain to the reader why they have chose the definitions they have, and how sensitive their results are to these choices.

It is somewhat concerning that the range of values displayed by the satellite measurements vastly exceeds that of the in situ data. The authors need to explain to what extent this is due to

the in situ data being fewer and spatially limited, and to what extent it is due to error in the satellite data. It is a concern that the classification might be based on erroneous values; it appears that according to the in situ measurements, water-masses 1 and 3 were not sampled. Comparison of the cruise track and Figure 9 indicates that the water mass 1 might never have been properly sampled by the CTD measurements, while it is a surprise that watermass 3 is never sampled in the MIZ on sections 7 and 8.

Can the authors put the cruise sections in context of the identified water masses?

Answer:
The range of variation in SSS and SST values covered by the satellite measurements (first row of Fig 8) is an order of magnitude larger than the one covered by in situ measurements (first column, bottom row of Fig 8). The difference in TS diagram covered by each type of measurement cannot be explained by the errors on satellite measurements (rms difference with respect to in situ measurements of 0.77°C and 0.8 in temperature and salinity respectively) nor by the uncertainties associated with each satellite product (Fig 4b and 5b). It primarily reflects the much better spatio-temporal monitoring of the different water masses by satellite measurements. This is now explained in the paper. We've chosen arbitrary limits and the number of water masses based on the distribution of T-S density points for the September 4, as it is shown on the figure 8. The T and S ranges of variation for each class has also been chosen to be well above the T and S uncertainties.
When we submitted the paper, we did not use any particular clustering method to separate the water masses, only the visual analysis of the potential centers of the water masses. Specially for this answer, I've just tested the dataset of SST&SSS for Sept 4 with the "Elbow method" used for the K-clustering to define the number of clusters centers (please, see details of the method here https://towardsdatascience.com/machine-learning-algorithms-part-9-k-means-example-in-python-f2ad05ed5203):

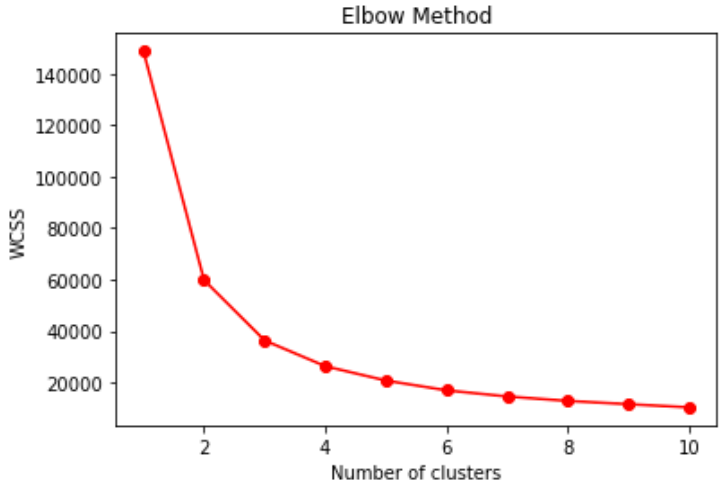

I propose that 6 cluster centers are acceptable for a classification, which main purpose was only to follow the transformation of the water masses. Any further analysis of the sensitivity will induce a number of rather heavy tests in terms of computational cost. A lower number of water masses will bring a less detailed picture of the transformation of the riverine water in the sea water, the sea ice melting and the beginning of freezing.
As for water masses 1 and 3 (both less saline than 25) absent in the CTD measurements, it is due to those simple facts, that:
1) the Arktika-2018 expedition didn't go far enough to the southern Laptev sea, close to the origin of the riverine water;

2) MIZ measurements show the presence of water mass 4, which is close to the WM3, but the WM4 is saltier. Indeed, there might have been 5 water masses, meaning one WM 3&4 together. We separated them mostly to be able to distinguish the water coming from the Kara Sea (seen on Aug 15 and Sept 25 in the west) and the freshwater to the east (in the East-Siberian Sea) exposed after the sea ice melting.

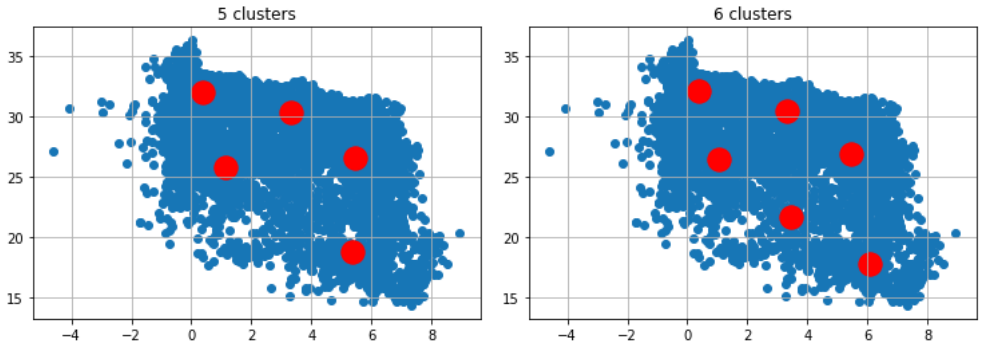

Minor points

P1L20 - make it clear exactly what region was affected by this freshwater decrease
Answer: Corrected to the Eurasian shelf

P2L14 - Statement should be revised in light of Osadchiev et al. 2020
Answer: The paper of Osadchiev was influenced by this paper sent for a review to OS in May 2019, one year before Mr Osadchiev decided that he also has some relevant data to publish on this subject. His comments on this work can be found in the Ocean Science Discussion in 2019. Considering this, this paper does not require to be referred to here, as apparently our "synoptic description of the Laptev Sea surface waters" was done before his publication.

Fig. 1 - Mark rivers clearly. Dotted lines are used for ice edge, bathymetry and grid markings; this is a bit hard on the eyes. Consider changing some (or all) of these to light, solid lines. Consider choosing a different colour for text that refers to different types of features (eg. rivers in blue, straits in red…)
Answer: the style of representation was slightly changed. The colour of the figure corresponds only to the time of both the expedition time measurements and the sea ice edge moment. Using different colours for geographical features would be misleading.

P5L7 - what exactly is the standard error in this context?

$$\sigma_{\bar{x}} \approx \frac{s}{\sqrt{n}}$$

σ is the standard deviation of the time series (temperature or salinity)
n is the size (number of observations) of the time series.

P6L1 - units can be given for the standard deviations

Answer: Added « degree Celsius ». Salinity is unitless following the recommendations of earlier reviewers.

P7L6 - what depth does the satellite sample? This is clearly relevant in the discussion here and would be worth stating explicitly.
Answer: The section dedicated to the satellite measurements is Section 2.2
For the SST blended product, the actual depth measured by the satellite is not very important, as 1) the IR and the MW wavelength are different and penetrate the surface on o(mm): 1 micro-m for IR and 1 mm for MW; in any case, the effect of skin-layer measured by the SST is supposed to be corrected in the product L4 and the temperature is supposed to be brought to the "foundation temperature" – the temperature of the surface layer not impacted by the diurnal cycle.
As for the SSS we talk about 1 cm. The effect of vertical stratification on the SSS validation is described thoroughly in Supply et al.,2020.

P7L8 - given that the median profile portrays a picture of the water column that is not representative of any given profile, I am not sure it is worth describing it here as if it is physical. For instance, the smoothness of the thermo-/halocline is an artefact of averaging many profiles with sharper halo-/thermoclines at different depths.
Answer:
We agree, but this figure was explicitly requested by one of 5 other reviews during the last 18 months of reviewing process

P7L14 - use 'is composed of' instead of 'composite' (composite suggests another meaning)
Answer: Thank you, corrected

P8L12 - meaning of statement in parentheses is unclear
Answer: We mean that the IR SST measurements can be obtained only in case of clear sky without clouds. Clouds are opaque for IR waves. Added "without clouds" to the text.

Fig. 4 - Contour plot looks a bit messy - consider pixel plot without contours. Fig. 4c does clearly show coherent groupings with distinct biases in the satellite data (e.g. measurements from days 45-50 are consistently too cold in satellite data, while in days 25-30 the satellite data are too warm)
Answer: Agreed. The blue points standing out for the days 45-50 correspond to the measurements in MIZ. Although DMI do their best to develop a special algorithm for the MIZ, it is still not perfect. This commentary is provided in P10L28-30

P9L6 - is this all data or just those from CTD casts where the mixed layer depth is below 7 m?
Answer: These are all measurements from all CTD casts.

P10L21 - 'potential cloudiness' is a bit confusing for a specific date that has already passed. Was it partially cloudy?
Answer: Yes, corrected

P10L33 - justification required, as suggested above
Answer: A "good agreement" is justified by a high correlation coefficient and independency of the error over the ice-free areas (excluding the MIZ).

P11L7 - provide a reference for this statement? It is not obvious to the reader that this would

be the case, as density of measurements and degraded sensitivity are not obviously compensating.
Answer: The SSS sensitivity decreases when the SST decreases, but the number of measurements increases when the latitude increases. Repeated measurements over the same area reduce the error when the seven-days running means are calculated (see Supply et al, 2020).

P11L20 - explicitly state the implications of oversampling for interpretation of the results
Answer: Each SMOS retrieved salinity is integrated over a 50km x 50km area. We don't make any spatial average. The oversampling on a 15km grid is possible owing to the image reconstruction of the SMOS interferometric data, but in our processing we don't make any spatial average.

P11L26 - is this an innovation or a convention? Provide a reference if a convention, provide justification if an innovation
Answer: It is a convention proposed to ignore the SSS with higher uncertainty values due to a too low or too high wind speed (see Supply et al, 2020 for details).

P13 L2 - DMI SST / SST DMI - be consistent with the naming
Answer: Thank you, corrected everywhere to DMI SST

P13L6 - quantitative assessment of what makes this a very good agreement would be valuable (as suggested above)
Answer: Comparison between the in situ practical salinity and SMOS SSS "A" shows a very good agreement, not yet demonstrated before by any other salinity product in the Laptev Sea: the correlation coefficient is 0.86 with a RMS = 0.86.

P13L24 - what exactly are 'the ice charts' from AARI? Are they available online?
Answer:
Ice charts show the sea ice concentration and type and are created from satellite data by an ice expert. Regional ice charts prepared in AARI can be accessed from http://www.aari.ru/odata/_d0015.php?lang=0&mod=1&yy=2018 or http://www.aari.ru/odata/_d0004.php?m=Lap&lang=0&mod=0&yy=2018

P15L9 - can thermal fronts be seen in the daily satellite data?
Answer: yes, as it is seen in Fig.4

P16L1 - provide uncertainty
Answer: The uncertainty for the Laptev sea is 0.0996 and for the East-Siberian is 0.1981

P16L11 - how might one distinguish between these two sources of variability? Can any attempt to do so be made here? Can a comparison be made with the variability detected in the observational survey?
Answer: It is rather difficult to estimate the SSS variability with point-CTD measurements. The only "point" close to MIZ, where measurements were done twice is a cross-section of CTD sections 6 and 8 (stations 79 and 108). Both stations are close to 154°E.

Station 79 was done on September 8, 2018; station 108 was done on September 17, 2018.

In 9 days, there is a difference in surface salinity of 0.5.
The edge of the MIZ at Station 79 coordinates (77.5N, 154.18E) was detectable with MODIS images on September 2 (See figure below) and Station 108 was done on the edge of MIZ later as well.
The main problem is that these data obtained in MIZ is certainly filtered out from the SMOS SSS measurements, as sea ice pixels elevated brightness temperature contaminates the salinity signal for retrieval.

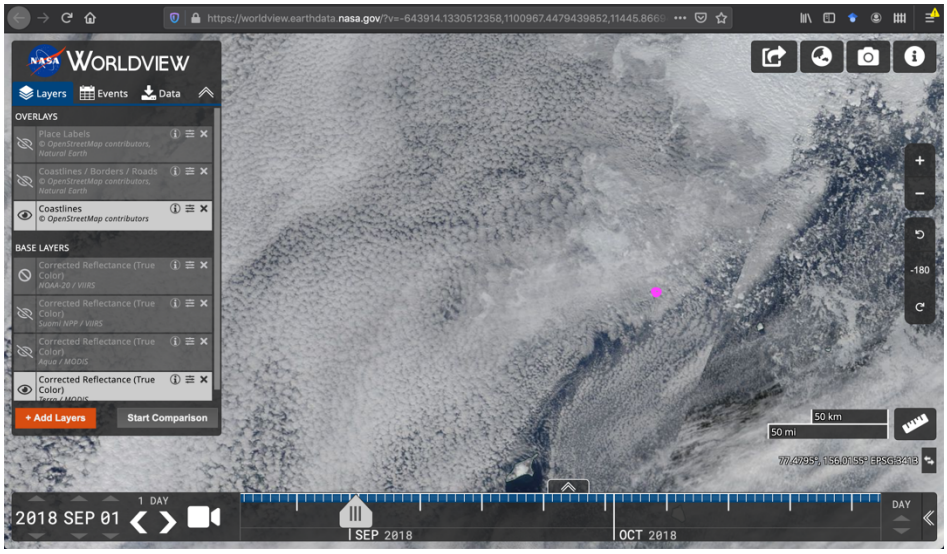

September 2, 2018 MODIS visual band: position of future Station 79 is marked with a magenta circle. The MIZ edge is seen below the clouds.

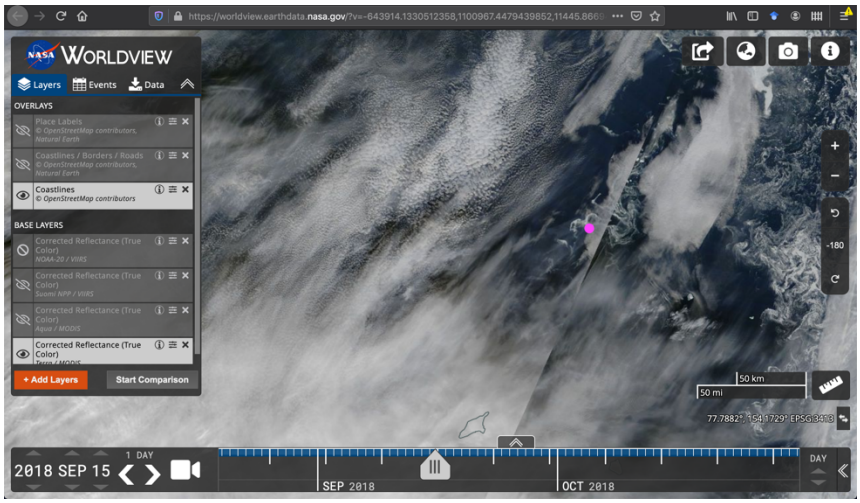

September 15, 2018 MODIS visual band: position of future Station 108 is marked with a magenta circle. The MIZ edge is seen below the clouds, the station is still in MIZ area.

P16L23 - explain origin of the two separate branches
Answer: The two surface branches are mostly the warmer and low-saline surface waters of the ice-free Laptev Sea and the colder and low-saline waters of the ice-covered East-Siberian Sea.

The latter correspond to the measurements from the section 7 and 8 eastward 150E (see the Figure below).

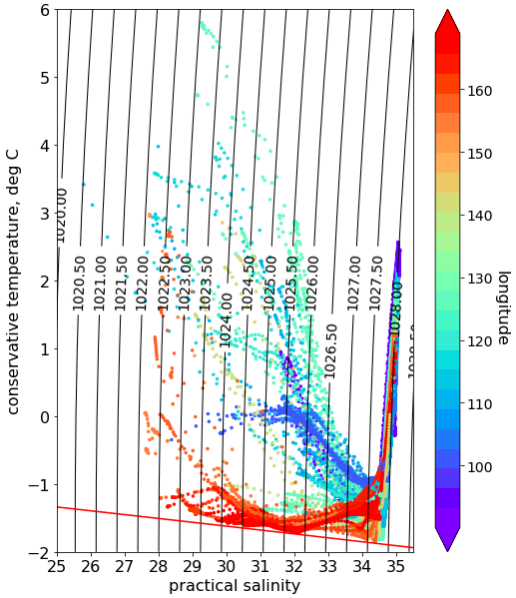

P16L29 - make it clear to the reader that these diagrams are not analogous to Fig. 7, as they are only for surface values
Answer: Corrected, thank you

P16L1 - describe how water mass boundaries were determined (as suggested above)
Answer: Corrected in the text.

P18L9 - worth explicitly stating that this water mass is not considered to be melt, but trapped river water, based on the geochemical analysis in 3.3.4
Answer: Thank you for the suggestion, corrected

P18L4 - clarification required to make origin of CMS as referred to in L4 and L14 compatible. Could be simply saying that

- it is comprised of both transformed CF and transformed WF (if this is the case),

or explicitly saying that

- there is no transformation route to CMS directly from WF, but it is produced only from CF.

Answer: Neither of these hypotheses apply.

- *CMS can be produced from WF by passing the stage WMS (if it is the "Lena river water" between the Laptev and the East-Siberian Sea.*
- *CMS can be a transformed river water from the Kara sea. And there we don't know was it first WMS or CF.*

Fig. 9 - use acronyms for the water masses as per main text
Answer: Corrected

P23L6 - it is not surprising that there is a weak correlation between these variables; salinity changes will effectively integrate the variability in the wind (see, for instance Osadchiev et al. 2020, Fig. 4). Could the authors try correlating the time derivative of salinity and temperature with the wind speed? This might be more instructive.

P24L5 - is it that the "warm" river water signal is not observed anymore?
Answer: Yes, this is what we meant. Corrected in the text.

Fig. 13 - show dashed blue line over entire sections for those done entirely in the MIZ
Answer: Corrected

P26L13 - comment on the implications of the findings regarding the B-V frequency?

Answer:
Corrected to:
« The maximum value of Brünt-Väisälä frequency are less than for other sections and are observed at 20 m depth and at 55 m depth, following 1024kg/m3 and 1026.5kg/m3 isopycnals, accordingly, showing the maximum stability of water vertical stratification under the ice »

P27L8 - comment on timing, which is naturally important here
Answer: Corrected to
« The sea ice formation (the negative values of sea ice melt fraction) is found in MIZ and its vicinity at 78-70°N - 150-160°E of the East-Siberian Sea, which is expected, as this measurements were done in the second part of September 2018, the beginning of freezing season. The presence of river waters may accelerate the sea ice formation if the air temperature favours it. »

P29L13 - sentence is ambiguous
Answer: Corrected

All figures showing maps should include the traces of the major rivers, and in my view it would be helpful to keep the names of the straits on at least one window in each figure.

Editorial

The written text needs some improvement in grammar. A few pointers: Use of ‘the’ and ‘a’ needs attention

Use of passive voice and tenses is sometimes confusing/ambiguous. I’d recommend using second person (‘we’), active voice, present tense to described things done by you, the authors, in this study.

Editor comments

Following up on Reviewer 4 “the” and “a”: “the” is the “definite article”, “a” is the “indefinite article”. That means that “the” is used when referring to something that has already been “defined”, either because already mentioned in the previous text or by an adjective, e.g. “the black cat” or “a cat” if you did not previously refer to cats.

Reviewer 1 commented on Ekman transport in shelf seas. There are two points.

a. Surface Ekman transports are relative to the flow beneath the surface layer. If the wind stress implies upwelling near a coast, for example, the offshore Ekman transport implies onshore flow below and the absolute offshore transport is reduced.

b. As hinted in a, the nearby coast can induce vertical velocity with uniform wind stress.

Properties of surface water masses in the Laptev and the East-Siberian Seas in summer 2018 from in situ and satellite data

Anastasiia Tarasenko[1, 2, 3], Alexandre Supply[4], Nikita Kusse-Tiuz[1], Vladimir Ivanov[1], Mikhail Makhotin[1], Jean Tournadre[2], Bertrand Chapron[2], Jacqueline Boutin[4], Nicolas Kolodziejczyk[2], and Gilles Reverdin[4]

[1]Arctic and Antarctic Research Institute, Saint-Petersburg, Russia
[2]Univ. Brest, CNRS, IRD, Ifremer, Laboratoire d'Océanographie Physique et Spatiale (LOPS), IUEM, Brest 29280, France
[3]now at Centre National de la Recherche Météorologique (CNRM), Université de Toulouse, Météo-France, CNRS, Lannion, France
[4]Sorbonne Université, CNRS, IRD, MNHN, Laboratoire d'Océanographie et du Climat, Expérimentations et Approches Numériques (LOCEAN), Paris, France

Correspondence: Anastasiia Tarasenko (tad.ocean@gmail.com)

Abstract. Variability of surface water masses of the Laptev and the East-Siberian Seas in August-September 2018 is studied using ~~in situ~~ *in situ* and satellite data. ~~In situ~~ *in situ* data were collected during the ARKTIKA-2018 expedition and then complemented with satellite-derived sea surface temperature (SST)~~and~~ , salinity (SSS), sea surface height, wind ~~speeds~~ speed, and sea ice ~~concentrations~~concentration. The estimation of SSS fields is challenging in high latitude regions, and the precision of Soil Moisture and Ocean Salinity (SMOS) SSS retrieval is improved by applying a threshold on SSS weekly error. ~~The~~ For the first time in this region, the validity of DMI (Danish Meteorological Institute) SST and SMOS SSS products is thoroughly studied using ARKTIKA-2018 expedition continuous thermosalinograph measurements and CTD casts. ~~The surface gradients~~ They are found adequate to describe large surface gradients in this region. Surface gradients and mixing of ~~river and~~ the river and the sea water in the ice-free and ~~ice covered~~ ice-covered areas are described with a special attention to the marginal ice zone at a synoptic scale. ~~The Ekman transport is calculated to better understand the pathway of surface water displacement.~~ We suggest that the freshwater is pushed northward, close to MIZ and under the sea ice, ~~as it~~ which is confirmed by the oxygen isotopes analysis. The SST-SSS diagram ~~using surface satellite estimates showed the~~ based on satellite estimates show a possibility to investigate the surface water masses transformation at ~~synoptic scales and reveal the presence of~~ a synoptic scale and reveal a presence of the river water on the shelf of the East-Siberian Sea. The Ekman transport is calculated to better understand the pathway of surface water displacement on the shelf and beyond.

1 Introduction

The eastern part of the Eurasian Arctic remains one of the less studied areas of the Arctic Ocean. **?** described this region as an "interior shelf" (~~Kara, Laptev,~~ the Kara, the Laptev, the East-Siberian, together with ~~Beaufort Seas~~the Beaufort seas), where 80% of the Arctic basin river discharge is released. **?** estimated the annual river water input as 2000 m^3. The Arctic Ocean stores 11% of a global river discharge, so its role in ~~the~~ a planetary water budget ~~merits attentionwith attention. Surface stratification~~

~~and~~ deserves a special attention. The surface stratification and the freshwater content are regarded as key parameters that have to be followed to better understand the changing state of a "New Arctic" climate (**?**). **?** discussed the salinification of the Laptev sea since 1989 up to 1997, explaining it by the eastward freshwater displacement and an excessive brine release in the sea ice leads. A more recent study reports that a 20% increase in the Eurasian river runoff is observed over the last 40 years (**?**). Overall, a freshening of the ~~Arctic Ocean in 2000-2010~~ American basin of the Arctic Ocean was reported in ~~the American basin~~ 2000-2010 (**?**), and at the same time, a decrease in a freshwater content of about 180 km^3 between 2003 and 2014 was calculated from altimetry measurements by **?** ~~. **?** discussed the salinification of the Laptev sea since 1989 up to 1997, explaining it by the eastward freshwater displacement and an excessive brine release in the sea ice leads~~over the Siberian shelf. The importance of shelf seas for the freshwater content storage and distribution was outlined in several recent studies (**?**, **?**, **?**)~~,~~ ~~and its exchange with the deep basins is apparent (~~. The importance of the exchange between the shelf seas ans the deep basin is large: 500 km^3 for the Laptev and the East-Siberian Seas with anticyclonic atmospheric vorticity, calculated from 1920-2005 hydrographic measurements "on quasi-decadal timescales" by **?**)~~.~~. Previously, the Arctic shelf was considered as a "short-term buffer" (3.5 ± 2 years) storing the river water before it enters into the deeper central part and is transported by the Transpolar drift (9-20 years) to the North Atlantic through the Fram Strait (**?**). A recent study of **?** shows that the "intensification of the hydrologic cycle" will speed up the transport of the freshwater, carbon, nutrients and trace elements from the shelf to the central Arctic and further: the trace elements and isotopes move from the shelf edge to the Transpolar drift stream over 3-18 months, and the Transpolar drift takes 1-3 years.

~~The processes occurring at the Eastern~~ Processes taking place on the eastern Eurasian Arctic shelf are important ~~, as~~ for the redistribution of ~~this freshwater coming into this region~~ the freshwater arriving there and its further path~~is still unclear and its amount is supposed~~ , while the amount of freshwater is expected to increase (**?**~~). Complex~~ , **?**). A complex topography, several sources of fresh and saline water masses, unstable atmospheric conditions and ~~other parameters, like~~ ocean processes, such as mesoscale activity and tidal currents, can alter the direction of ~~this~~ the freshwater distribution. Close to the coast the riverine water from several sources is ~~considered~~ expected to propagate eastward as a "narrow (1-20 km) and shallow (10-20 m) feature" (**?**, **?**), but its transformation and mixing with ~~saline sea water~~ a saline seawater and sea ice melting and freezing ~~is~~ are less studied. The Laptev ~~Sea~~ and the East-Siberian shelf areas were described as a substantial region of sea ice production for the central Arctic (**?**), and to better ~~understand~~ estimate the impact of the incoming freshwater on the sea ice formation, the freshwater pathways in the Arctic should be ~~understood better~~ better understood. Despite several studies on the freshwater in the Eastern Arctic (e.g., **?**, **?**, **?**, **?**), to the best of our knowledge, no study has shown yet the evolution of the water masses on a synoptic scale in the Laptev Sea. In this paper, we look at the information accessible with satellite salinity. The salinity provides precious information about the fate of the freshwater river input. While this information is restricted to the top sea surface, the regular and synoptic monitoring of sea surface salinity from space allows to document its spatio-temporal variability in great details not accessible with any other means, providing a new tool for analyzing some of the processes at play.

The Laptev Sea is shallow in its southern and central parts (less than 100 m) with a very deep opening in the north (3000 m) (Fig. 1). Several water masses are mixed in the Laptev Sea. The Lena, ~~the Khatanga, the Anabar, the~~ Khatanga, Anabar, Olenyok, and ~~the Yana Rivers~~ Yana rivers discharge fresh water in the shallowest part of the Laptev Sea in the south. The Kara

Sea water enters via the Vilkitskiy and the Shokalskiy straits, the Atlantic Water (AW) propagates along the continental slope to the north of the Severnaya Zemlya Archipelago and further eastward, the Arctic Water ~~exists in the~~ is found in its northern part (**?**, **?**, **?**). ~~The direction of~~ A direction of the surface freshwater circulation is supposed to correspond to ~~the~~ a general displacement of the intermediate Atlantic Water: mainly eastward following the coastline (**?**). This eastward transport brings the water masses of the Laptev Sea over the shelf of the East-Siberian Sea where ~~it comes under the additional influence of Pacific-derived~~ they meet Pacific-origin waters (**?**, **?**).

In the Arctic region, a strong seasonality of air-sea heat ~~fluxes with~~ flux, sea ice melting and freezing modify ~~temperature and~~ the temperature and the salinity in the upper layer, and therefore, result in a ~~complicated~~ vertical structure of the water column with fronts at the surface and "modified layers" in the interior (**?**, **?**, **?**). The most common concept of the upper ocean layer is a "mixed layer" concept: between ~~the~~ an ocean surface being in contact with the atmosphere and a certain depth, ~~temperature and~~ the temperature and the salinity are homogeneous. ~~It~~ A mixed layer extends until a specified vertical gradient in density and/or temperature (**?**, **?**), or ~~the~~ a maximum of Brunt-Väisälä frequency (**?**). In the Arctic, the reported mixed layer depth (MLD) ~~vary~~ varies between 5 and 50 m depending on region, time, and open water or under the ice measurements (10 m in the Laptev and the East-Siberian ~~Seas~~ seas and 5 m in the Central Arctic ocean and Northern Barents Sea in summer, **?**; 10-15 m in the Beaufort Sea close to MIZ in summer, **?**; 20 m in the Barents Sea in late summer, **?**, 40-50 m under the ice close to the North Pole in winter, **?**).

At the same time, **?** proposed to use ~~the~~ a term "surface layer" instead of "mixed layer" for the Arctic Ocean, because ~~the~~ a water layer lying between the sea surface and the Arctic main halocline can be weakly stratified even though the halocline hampers an active exchange of matter and energy. The main halocline is situated at 50-100 m depth in the Eastern Arctic (**?**), and at 100-200 m depth in the Western Arctic Ocean (**?**). Using ~~the concept of~~ concept of the "surface layer"~~with some assumptions~~, the processes in that layer can be discussed separately from the ones in the deeper layer. The freshwater is ~~supposed~~ expected to be delivered to the central (European) Arctic from the Siberian shelf, roughly along the Lomonosov Ridge and to the western Arctic, partly along the continental slope ~~.~~ (**?**).

The position of the pycnocline in the Arctic is mostly defined by ~~the~~ salinity. One of the first studies of **?** devoted to the freshwater content was using 34.80 as a reference salinity value separating the "fresh" and the "saline" water; 34.80 was considered ~~the~~ a mean Arctic Ocean salinity at that time. This value is used as well in more recent overviews (e.g. **?**, **?**) ~~,~~ and helps to define the "Atlantic Water" as saltier than this value. **?** used a ~~depth of 34 isohaline to estimate the~~ 34-isohaline depth to estimate a liquid freshwater content in the Arctic Ocean. **?** considered ~~the depth of~~ a depth of a "near-freezing freshwater mixed layer" in the Eurasian Arctic Ocean to be 5-10 m. **?** reported an overall salinity in the upper 5-50 m layer within the range from 30.8 to 33 based on ~~in situ~~ *in situ* data in the Laptev Sea during 1950-1993 and 2007-2012. Between the very surface layer and the Atlantic Water, **?** found ~~a~~ the Modified "Lower Halocline" Water with typical characteristics of salinity (between 33 and 34.2) and a negative temperature (below -1.5°C); in 2002-2009 this layer was situated at 50-110 m depth. The study of **?** on the Arctic Ocean freshening defined the upper ocean layer to be between 0 m and a depth of a density layer $\sigma_\theta = 27.35\ kg \cdot m^{-3}$. This isopycnal is often located at 140–150 m depth, "slightly above the Atlantic Water upper boundary defined by the 0°C isotherm".

The stable vertical stratification is modified by mixing. Mixing can be induced by winds generating surface-intensified Ekman currents, mesoscale dynamics (eddies), a shear in tidal and other currents (**?**, **?**, **?**). ~~The tidal~~ Tidal currents and internal waves amplified over the shelf edge are associated with the mixing in the interior of the water column, below or in the main Arctic pycnocline (**?**, **?**, **?**).

Temperature and salinity fronts separate well-mixed water masses. **?** and **?** showed that interannual changes of a river discharge and wind patterns define the position of ~~the~~ oceanographic fronts in the central part of the Laptev Sea. Based on ~~the~~ model results, **?** showed that in 1989-1997 the freshwater was driven eastward under the influence of winds associated with a "strong cyclonic vorticity over the Arctic". The same study demonstrated that the associated salinification of the central Arctic Ocean ~~weakens~~ weakened the vertical stratification of the water column. The anticyclonic regime is considered to increase the salinity of the shelf seas (**?**). **?** discuss the importance of sea ice, as it creates a surface drag and establish the Ekman transport of the freshwater in the surface layer, which, in turn, impacts the dynamical ocean topography and geostrophic currents in the Arctic Ocean. **?** further ~~mentioned~~ mention that alongshore winds correlated with AO (Arctic Oscillation) index create the onshore Ekman transport, changing ~~the~~ water properties over the shelf.

~~Concerning the seasonal dynamics, the summertime~~ In the seasonal cycle, the summer season is of a particular interest for all Arctic studies. The sea ice melting usually starts in June and ends in August-September, while the sea ice formation can start already in September, and by November the Laptev Sea is ~~covered completely~~ already completely sea-ice covered. The East-Siberian Sea is ~~covered by~~ usually covered by the sea ice most of the year, and is exposed to the air-sea interaction for a shorter period of time (in August-September) over a smaller ice-free surface than the Laptev Sea. August and September are two summer months that are very important for the heat exchange between the open ocean and the atmosphere over the Laptev Sea. In a recent study, **?** reported that during this time period when the sea ice is melting and the ocean is opening, the net radiative balance at the sea surface changes from 100 W/m^2 to zero values, following the seasonal cycle of shortwave radiation (meaning the flux from the atmosphere to the ocean). The sea level anomalies over the Eastern Arctic shallow seas are positive and largest in summer (up to 10 cm at 75°N, down to 3 cm at 80°N, as it was reported by **?**). The seasonal peak of the maximum freshwater content over the shelf is found in summertime when the river discharge is the highest, while the freshwater content minimum (meaning the export of this accumulated freshwater) occurs in March, when the freshwater captured by sea ice is advected away from the shelf (**?**, **?**).

The Laptev Sea is not at all sampled by Argo products, so the recent ARKTIKA-2018 expedition measurements combined with novel satellite sea surface salinity and other satellite-derived parameters provide an unprecedented documentation of the temporal evolution of the surface water properties in the Laptev and East-Siberian Seas during the summer 2018. In this study, we propose to follow the upper ocean water displacement and to discuss what causes it on a daily basis.

2 Data and Methods

To analyse the upper-ocean processes, we will focus on the ~~very surface~~ surface layer with satellite data and on the upper 250 m layer with the CTD (conductivity, temperature, depth) casts, ~~showing~~ providing the isohaline and isopycnal positions.

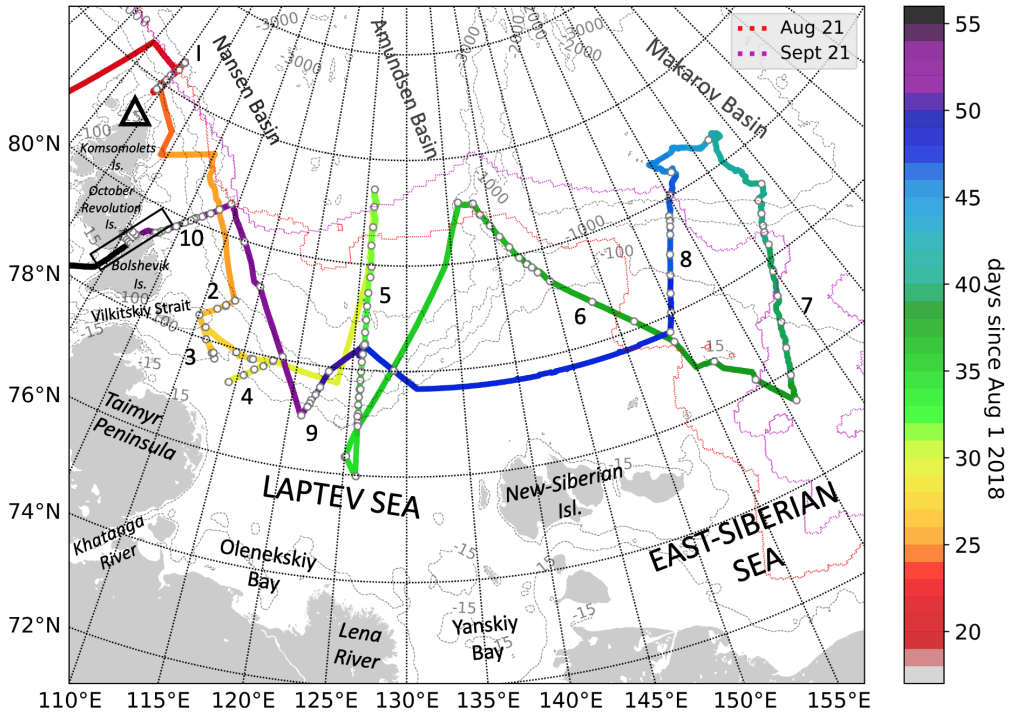

Figure 1. Legs and stations of the ARKTIKA-2018 expedition overlayed on the bathymetry from ETOPO1 "1 Arc-Minute Global Relief Model" (**?**). CTD stations are shown with white dots. The ~~color~~ colour indicates the number of days since August 1, 2018. The sea ice edge position is indicated with a red dashed line for the beginning (August 21) and with the purple dashed line for the end of the expedition (September 21). The ice edge is based on the sea ice mask provided in the ~~SST~~ DMI SST product. Numbers indicate positions of 10 oceanographic transects discussed below. The black triangle in the north of the Komsomolets Island shows the Arkticheskiy Cape. The Severnaya Zemlya Archipelago consists mainly of the Komsomolets, the October Revolution, and the Bolshevik Islands (with smaller islands not shown here). The black box indicates the Shokalskiy Strait between the October Revolution and the Bolshevik Islands. The Yana river estuary is situated southward the Yanskiy Bay (out of the map).

Such an approach to the upper layer is required to estimate the upper ~~of~~ limit of the Atlantic Water, which is one of the key contributors to the water mass transformation. The surface water evolution of the Laptev and the East-Siberian Seas is described and ~~analysed considering~~ discussed with respect to changes in wind speed and direction during the ARKTIKA-2018 expedition.

2.1 In situ measurements during the ARKTIKA-2018 expedition

Oceanographic measurements during the ARKTIKA-2018 expedition on board RV Akademik Tryoshnikov started on August 21, 2018 and ended on September 24, 2018 (Fig.1). Oceanographic sections were organized to take into account the ~~interests~~ requirements of different scientific expeditions on board, NABOS (Nansen and Amundsen Basin Observational System) and

CATS (Changing Arctic Transpolar System) to observe shallow and continental slope processes. NABOS sections were mostly cross-shelf (1, 5, 6-8, 10), and CATS sections were shallower (2-4, 9). ~~Section~~ Sections 3 and 10 were made in the straits between the Kara and the Laptev Sea: ~~the~~ section 3 in the Vilkitskiy Strait southward to the Bolshevik Island, with depths from 70 to 200 m opening into the deep central part of the Laptev Sea (more than 1000 m) and ~~the~~ section 10 in the narrow and rather shallow (250 m) Shokalskiy Strait between the Bolshevik and the October Revolution Islands. Some measurements were carried out in marginal ice zone (MIZ) and ice-covered area (see the sea ice edge positions at the beginning and the end of the cruise in Fig.1). In this study we define MIZ as an area with 0-30% sea ice concentration close to the ice edge. Standard oceanographic stations (145 in total) were conducted with SeaBird SBE911plus CTD instrument equipped with additional sensors. For this study, we use mainly the CTD measurements of potential temperature and practical salinity, but also the results of oxygen isotope analysis from the first (surface) bottle samples (**?**). All CTD data were processed and quality checked. The cruise data can be found at https://arcticdata.io/catalog/data (**?**) and **?**.

The ship was equipped with an underway measurement system Aqualine Ferrybox, widely known as a thermosalinograph, TSG. The instrument had a temperature and a conductivity (MiniPack CTG, CTD-F) sensors and a CTG UniLux fluorometer installed; thus, continuous temperature, salinity and chlorophyll-a estimations were obtained along the ship's trajectory. The inflow is situated at 6.5 m below the surface (the inflow hole is on the ship's hull). All data were processed and filtered for random noise and bad quality measurements, and then compared and calibrated with CTD measurements. When calculating a linear regression between CTD measurements at 6.5 meters depth and TSG measurements, we obtain a good correlation for both temperature and salinity (correlation coefficient equal to 0.979 and 0.966, respectively, not shown). The standard error is 0.023 for temperature and 0.025 for salinity, and the standard deviation for the difference of measurements (CTD minus TSG) was ~~$STD_{temp} = 0.413$~~ $STD_{temp} = 0.413°C$, and $STD_{sal} = 0.423$. To adjust the continuous TSG measurements to the more precise CTD measurements, we applied the obtained linear regression equation to TSG data. We only use these adjusted temperature and salinity data.

The vertical profiles of the conservative temperature and practical salinity in the upper layer are presented in Fig.2. To investigate if the TSG measurements can be used to study the surface layer in a highly stratified Laptev sea, we calculated a summer mixed layer depth following **?** method based on density and temperature gradient thresholds (Fig.2, a, c). The MLD is found at a depth of the first maximum temperature gradient below a depth of defined (by given threshold) density gradient (see **?** for details). Using the same approach, we computed MLD with density and salinity vertical profiles. The threshold chosen for practical density gradient was 0.3 kg/m^3 per 1 m, and 0.2 salinity units per 1 meter for conservative temperature and practical salinity gradients. Regarding the MLD calculated from salinity (MLD_{sal}), most of the measured vertical profiles (75.17%) had the MLD_{sal} below 7 m depth with the median of MLD_{sal} 11.99 m. As for the temperature (MLD_{temp}), 81.37% of the measured profiles had the MLD below 7 m depth with a median of $MLD_{temp} = 13.50m$. Thus, in most cases the upper 12 m of the surface layer was homogeneous, and ~~our~~ the CTD and TSG measurements can be used for the validation of satellite data. The median vertical profiles of temperature and salinity in the upper 5-100 m are presented as well as the associated STD in Fig.2, b, d). We observe rather cold (0.5°C) and fresh (30.5) water at 5 m, followed by a smooth thermo- and halocline down to 30 m depth (with a temperature of -1.3°C and salinity of 33.8). Below 30 m the temperature is slightly rising to -1 °C, and

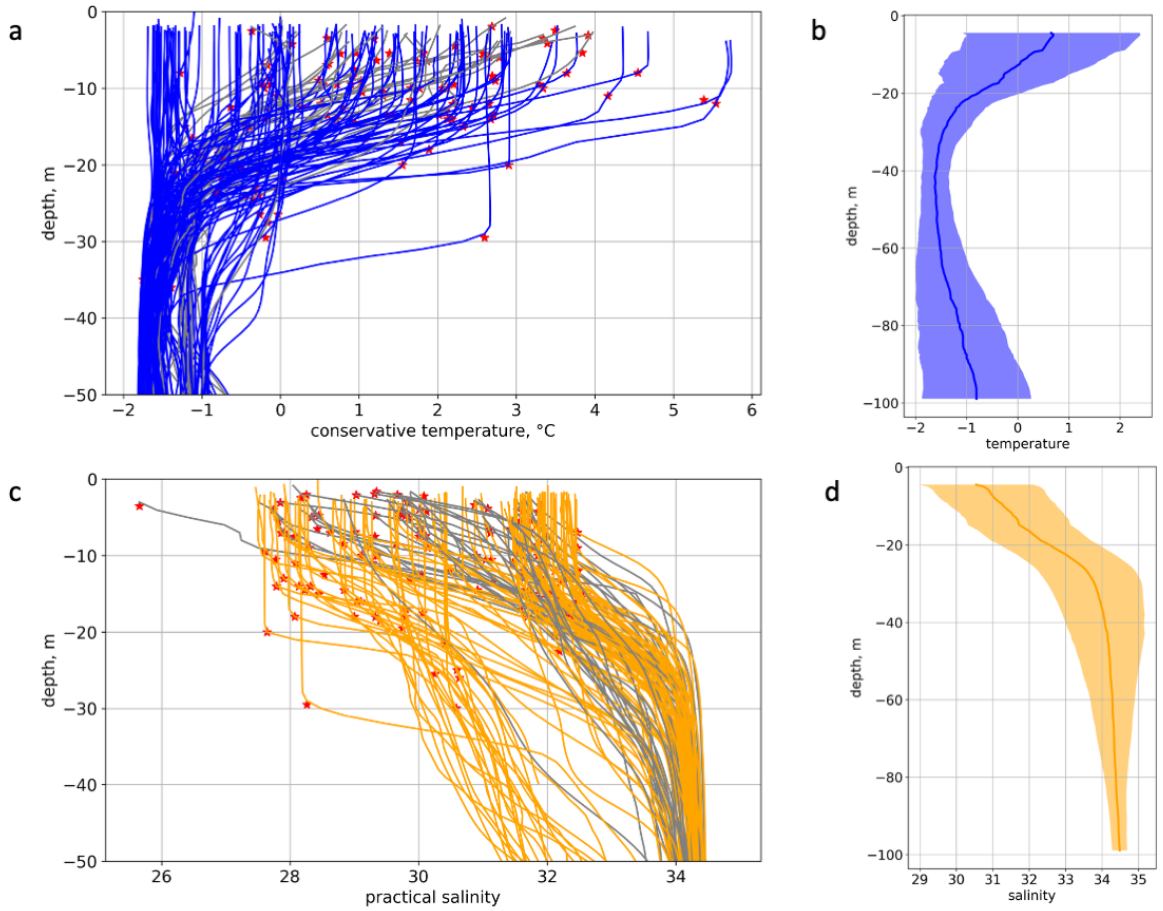

Figure 2. Vertical profiles of conservative temperature (a, b) and practical salinity (c, d) from CTD measurements in the upper ocean layer. Figures (a) and (c) show all vertical profiles in the upper 50 m, ~~where red stars indicate the mixed layer depth,~~ calculated using **?** method (see details in the text), ~~colored~~ red stars indicate the mixed layer depth; coloured profiles show the cases, when the MLD is below 7 m depth and gray profiles indicate when the MLD is above 7 m depth. Figures (b) and (~~c~~d) show the median vertical profiles ~~of temperature and salinity~~ in the 5-100 m layer of temperature and salinity, respectively, where the shaded area shows the associated STD.

salinity stays close to 34.5. The STD of conservative temperature is the largest at the surface (1.55°C) and smallest at 40 m depth (0.27°C). The STD of salinity is also the largest at the surface, 1.50, but is diminishing with depth to 0.20 at 100 m. Nevertheless, it is clear that at the end of a summer season in the region with very different water origins, these median profiles are not representative for all water masses. Additionally, we did an important number of CTD casts in very shallow areas with depths between 30 and 50 m, so the calculated averaged (median) vertical profile is ~~a composite~~ composed of "shallow" and "deep" vertical profiles. We do not include the very surface measurements above 5 m, because we ~~had only~~ only had 45 CTD measurements at 2 m depth among 146 possible, and taking them into account would bias the median profiles as well.

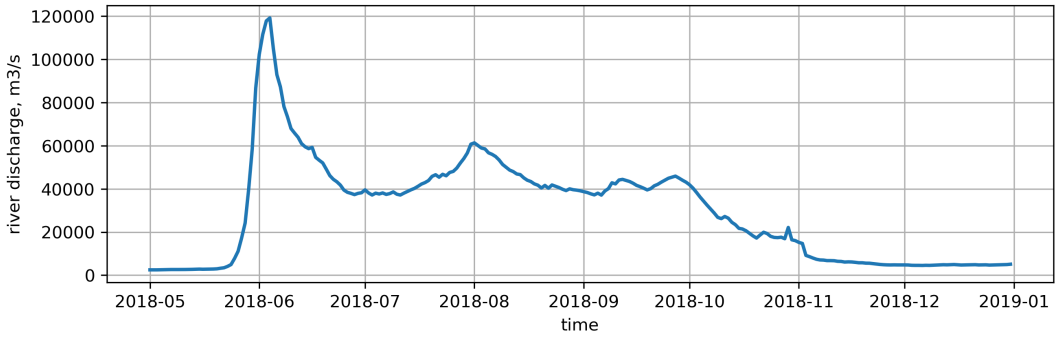

Figure 3. The Lena River discharge in 2018, data from Arctic GRO dataset (https://www.arcticrivers.org/data)

2.1.1 River discharge

To illustrate the amount and temporal variability of the river discharge in 2018, we used daily measurements of the Lena River discharge from the Arctic Great Rivers Observatory (GRO) dataset (https://www.arcticrivers.org/data)). In Fig.3 we present a time series of the Lena River discharge from May to November 2018. The river stayed under the ice with a very small discharge up to the end of May. The main peak of the Lena River discharge occurred in the beginning of the Arctic summer in June and corresponds to the snow and ice melting over the river basin in Siberia. In two weeks, the discharge changed from 2 500 to 120 000 m^3/s. The second, smaller peak of the river discharge occurred ~~in~~ at the beginning of August (60 000 m^3/s), which might be associated with the summer precipitation. ~~In~~ During August 2018 the river discharge ~~was decreasing~~ decreased from 60 000 to 40 000 m^3/s, and in September it varied very little staying close to 40 000 m^3/s. A significant diminution of the river discharge started in the beginning of October and continued up to the beginning of November. After the beginning of November the river discharge was very weak and close to its minimum values (4500 m^3/s).

The described seasonal dynamics is typical for the Lena River and consistent with existing results, e.g. demonstrated in **?**. It can be complemented by the results of **?** study of the large Siberian rivers using satellite data. **?** showed that the maximum of precipitation over the basins of the Lena, the Ob' and the Yenisey Rivers occurs in July, and the mean monthly air temperature is maximum at ~~this~~ that time.

2.2 Satellite data

Satellite data provide ~~an instant information about~~ information on the surface distribution of geophysical characteristics over the whole study area together with their temporal evolution.

All products listed below are considered from August 1, 2018 to September 25, 2018 (the last day of ARKTIKA-2018 expedition). For consistency, when not specifically indicated all products are linearly interpolated on a regular grid within the ~~bounding~~ box 74-85N 90-170E, with 0.01~~degree~~ -degree step in latitude, and 0.05 degree in longitude. The spatial resolution of the selected grid roughly corresponds to 1 km.

2.2.1 Sea surface temperature

The SST-retrieving instruments with the highest resolution, such as AVHRR (Advanced Very High Resolution Radiometer), MODIS (Moderate Resolution Imaging Spectroradiometer) and VIIRS (Visible Infrared Imaging Radiometer Suite) work in Near Infrared (NIR) and Infrared (IR) bands and strongly depend on atmospheric conditions (providing measurements for clear sky without clouds). For lower resolution microwave instruments, such as AMSR2 (Advanced Microwave Scanning Radiometer 2), the clouds are transparent, but the SST retrievals may still be hampered by high wind speed and precipitation events. As satellite measurements in IR and NIR ranges are sparse because of the frequent cloudiness over the Arctic Ocean, we used a blended product. In this paper we use the Danish Meteorological Institute Arctic Sea and Ice Surface Temperature product (hereafter referred as "~~SST DMI~~ DMI SST"). ~~SST DMI~~ DMI SST is a Level 4 daily product provided by the Copernicus Marine service ("Level 4 product" means that several swath measurements were interpolated to achieve a regular resolution in time and space). Daily surface temperatures over the sea and ice are derived on a 5 km spatial grid from several instruments: AVHRR, VIIRS for SST and AMSR2 for sea ice concentration, using optimal interpolation (**?**).

Besides the full coverage over the studied area, the advantage of the blended ~~SST DMI~~ DMI SST product is that it takes into account the ice temperature, so the marginal ice zone (MIZ) is better represented and not masked out. The total number of SST measurements ingested over the studied area from August 1 to September 25, 2018 varies from 1000 to 2500 measurements per pixel.

2.2.2 Validation of ~~SST~~ DMI SST

The first step of the ~~SST DMI~~ DMI SST validation was its value-by-value comparison with a collocated ~~in situ~~ *in situ* dataset (nearest neighbour ~~SST DMI~~ DMI SST pixel). For this analysis, we ~~co-embarkinglocated SST DMI with the in situ~~ co-located DMI SST with the *in situ* potential temperature measurements in the upper 6.5 m layer: all available CTD measurements averaged every half a metre above 6.5 m depth and all TSG measurements at 6.5 m depth averaged every 30 minutes. The median depth of the collocated CTD measurements is 5.25 m. As for the TSG, the ship was moving with a median speed of 8 knots during the cruise, so an average of 30-minutes TSG measurements is an average over approximately 7.5 km. Thus, 30-minutes TSG average is comparable with one ~~SST DMI~~ DMI SST pixel (10 km). There were 1707 collocated points in the analysis.

Although ~~, in fact,~~ satellite SST estimates may differ from the ~~in situ~~ *in situ* temperature measurements in the upper 6.5 m, we expect ~~some~~ an overall consistency between the datasets. Studies carried out by **?** devoted to the validation of MODIS SST in the MIZ, and by **?**, which described ~~in situ~~ *in situ* measurements in the iced-covered area, reported that the first 7-10 m layer below the surface was mostly homogeneous. As ~~it~~ is shown in Fig.2, most of our measurements (more than 75%) were homogeneous in the upper 12 m (and were done in the ice-free areas). Nevertheless, a diurnal warming and a local vertical mixing can affect the vertical temperature distribution in the very surface layer. The SST diurnal amplitude can reach more than 3 K in the Arctic Ocean (**?**). To create ~~SST DMI~~ DMI SST L4 product, only the observations between 21:00 and 7:00 local time are used (**?**), thus ~~,~~ local diurnal variations of SST are supposed to be filtered out. Diurnal variation of temperature

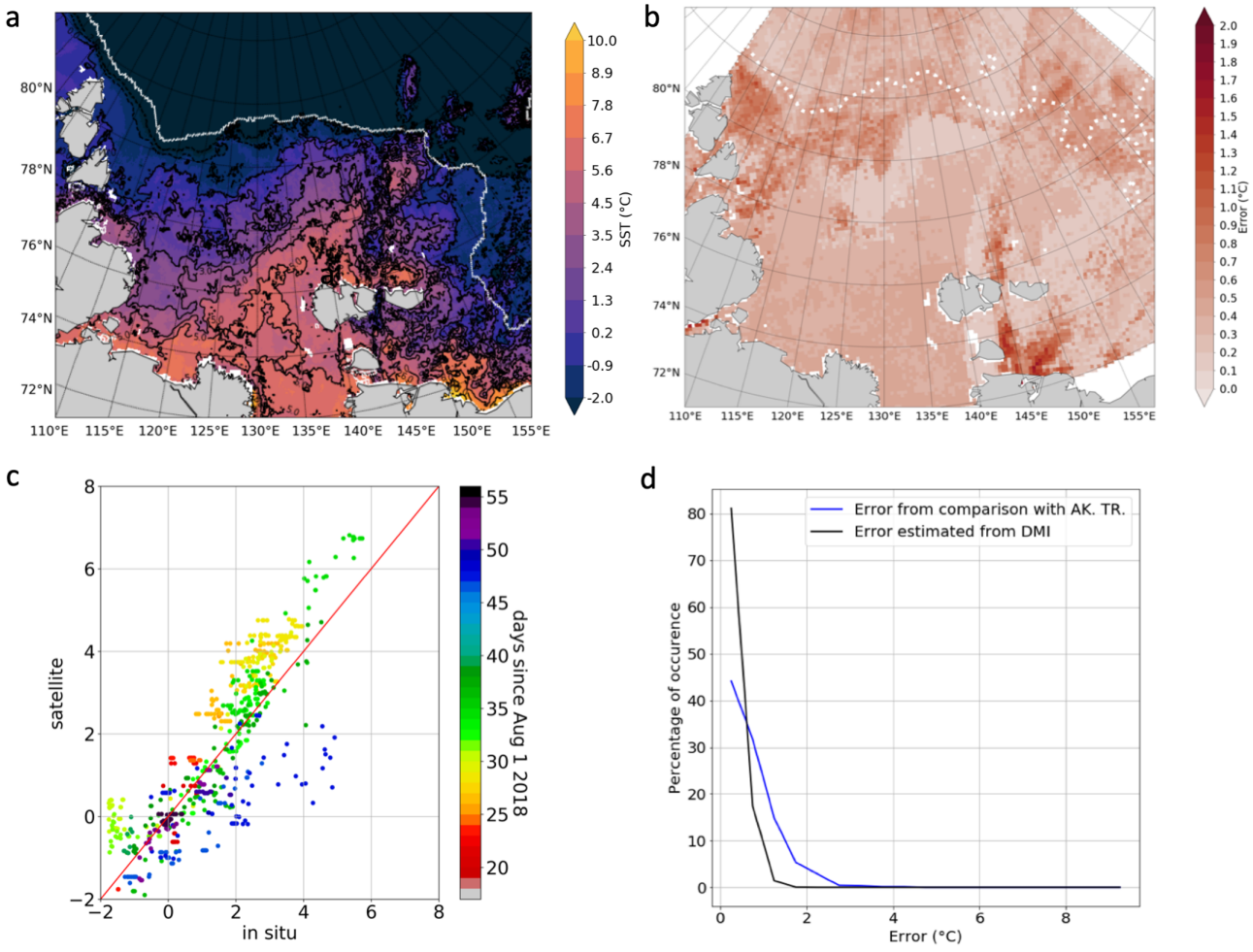

Figure 4. Sea surface temperature validation: example of ~~SST~~ DMI SST L4 image for September 13 (a) with the error estimates (b); comparison of collocated SST and ~~in situ~~ *in situ* data (CTD and TSG) in the upper 6.5 m (c) and distribution of ~~error~~ uncertainty provided by DMI and absolute difference derived from comparison with ~~in situ~~ *in situ* data (d).

might be present in real ~~in situ measurements in case of~~ *in situ* measurements during strong diurnal warming events, but no particular observations allowing to investigate this question were done during the cruise.

To illustrate the consistency of SST and ~~in situ~~ *in situ* temperature datasets, September 13, 2018 was considered as it was one of the rare days in summer 2018, when the central part of the Laptev Sea was cloud-free, which is especially important for ~~SST DMI~~ DMI SST.

The ~~SST DMI~~ DMI SST product for September 13, presented in Fig. 4 (a) shows a rather complex pattern with a pronounced gradient associated with warm river water in the central part of the Laptev Sea. The ~~error~~ uncertainty in SST estimates provided

by DMI, is shown in Fig.4 (b, d). The percentage of occurrence is computed in temperatures classes ~~with a size of~~ by 0.5~~degrees that starts~~ °C classes starting at 0~~degrees~~ °C(Fig.4, d). The highest ~~potential error~~ uncertainty (up to 2.5°C), was observed over some open sea areas ~~(due to potential cloudiness)~~that were partially cloudy, but was mostly associated with the sea ice due to its heterogeneity (Fig.4 (b)). Over most of the southern and the central part of the ice-free Laptev and the East-Siberian Seas, the ~~error~~ uncertainty is below 0.5°C and over the eastern part, it is below 1°C.

Comparison of the ~~SST DMI and in situ~~ DMI SST and *in situ* surface-layer temperature (Fig. 4, c) shows a ~~very~~ good agreement almost independent on area and time during the ARKTIKA-2018 expedition. The correlation coefficient is 0.89, and the RMS difference is 0.77°C. The difference between mean ~~in situ and mean SST DMI data is -0.19~~DMI and mean *in situ* surface temperature data is 0.19°C~~, where the SST DMI is higher than the in situ temperature. This value~~ . This excess average DMI SST seems to be ~~realistic, as the CTD data justifies it. According to CTD measurements,~~ possible, based on CTD measurements, indicating that the 0-3 m water layer is on average 0.3°C warmer than the 3-6.5 m layer (not shown). The largest deviations are observed when the ~~expedition is working~~ ship is in the MIZ or a more compact sea ice, so they might be associated with either imperfect sea ice flagging of some stages of sea ice in the ~~SST DMI~~ DMI SST product or a noise introduced after re-interpolation of data on a regular grid. This noise together with the different sampling of ~~in situ~~ *in situ* potential temperature measurements and ~~SST DMI~~ DMI SST product lead to a ~~standard deviation of the difference between in situ and SST DMI larger than the error~~ distribution of the absolute differences between *in situ* and DMI SST slightly wider than the one of uncertainties provided in the ~~SST DMI~~ DMI SST product (Fig. 4, ~~lower right). Overall, SST DMI agrees well with in situ data,~~ d). Nevertheless, this comparison should be taken only as indicative of a reasonable order of magnitude of the uncertainties given the limited number of *in situ* measurements for each uncertainty range. Overall, DMI SST agrees rather well with *in situ* data, and it captures a small-scale spatial variability of the SST in the ice-free areas (Fig. 4, a) well above SST uncertainties, so we use this product for the following analysis of SST time-series.

2.2.3 Sea surface salinity

Soil Moisture and Ocean Salinity (SMOS) is the first satellite mission carrying an L-band (1.41 GHz) interferometric microwave radiometer, which measurements are used to retrieve the sea surface salinity (SSS). With the recent processing, the standard deviation of the differences between 18-day SMOS SSS and 100-km averaged TSG surface salinity measurements is 0.20 in the open ocean between 45°N and 45°S (**?**). However, the precision degrades in cold water as the sensitivity of L-band radiometer signal to SSS decreases when SST decreases, even though this effect on temporally averaged maps is partly compensated by the increased number of satellite measurements at high latitude (**?**). A possibility of using SSS estimates in cold regions derived from L-Band radiometry has been ~~demonstrated recently~~ recently demonstrated by several working groups (**?**, **?**, **?**). However, existing L3 ("Level 3" means a product resampled at a uniform time-spatial grid, different from swath grid) SSS products: SMAP CAP/JPL (Soil Moisture Active Passive satellite, a product created using the Combined Active Passive algorithm by Jet Propulsion Laboratory) SSS or SMOS BEC (Barcelona Expert Center) SSS, are spatially averaged from 60 km to more than 100 km.

SMAP REMSS (Remote Sensing Systems) SSS L3 v3 provides a 40 km resolution version, but do not provide a sufficient cov-

erage in the Laptev Sea. The methodology developed in this study to retrieve SMOS SSS aims at maintaining SMOS original spatial resolution and at retrieving SSS as close as possible to the ice edge.

A new product, hereafter SMOS SSS "A" ("A" for the Arctic Ocean) L3, investigated in this study was computed using SMOS L2 ("Level 2" product means that a geophysical parameter, eg. SSS, was computed at the swath grid) SSS from the ESA (European Space Agency) last processing (v662, **?**)~~.~~, (Fig. 5, a). SMOS L2 SSS are available on the ESA SMOS Online Dissemination website. ~~The mean spatial (radiometric) resolution of~~ SMOS SSS are representative of SSS integrated over about 50x50 km^2 given the footprint of SMOS radiometric measurements involved in the SSS retrievals. The SMOS ~~product is close to 50 km, but SMOS~~ ESA L2 SSS products are oversampled over an Icosahedral Snyder Equal Area (ISEA) grid at 15 km resolution. The oversampling on a 15 km grid is possible owing to the image reconstruction of the SMOS interferometric data, but in this processing we don't make any spatial average for SSS fields.

SMOS "A" SSS was obtained as described below. Seven-day running means were computed for each day and each pixel of the ISEA grid, with a temporal Gaussian weighting function with a standard deviation of 3 days. The full width of SMOS ascending and descending orbits swaths was considered in order to take advantage of better temporal and spatial sampling over the Arctic Ocean and to decrease the uncertainty with temporal averaging. In order to eliminate the SSS at very low and high wind speeds because of ~~its high~~ higher uncertainties, SMOS ESA L2 SSS was considered only if the associated ECMWF (European Centre for Medium-Range Weather Forecasts) wind speed was between 3 and 12 m/s. SMOS ESA L2 SSS measurements were also weighted relative to the ~~estimated error~~ uncertainty of the SSS measurement (as in (**?**, equation A7). This ~~error~~ uncertainty was derived from ~~the SSS theoretical error~~ information provided with the SMOS L2 products, the SSS "theoretical error", derived from the uncertainty of all the parameters used for retrieving SMOS SSS, multiplied by the normalized χ^2 cost function of the SSS retrieval. **?** showed that the **?** dielectric constant model was inaccurate at low SST. In order to mitigate this effect, a SST-dependent correction derived from ~~the~~ Fig. 16 of **?** (blue-circle line) was applied: $SSS_{SMOS-"A"} = SSS_{SMOS-ESA-L2} - (-5 \cdot 10^{-4} \cdot SST^3_{ECMWF} + 0.02 \cdot SST^2_{ECMWF} - 0.23 \cdot SST_{ECMWF} + 0.69)$. Finally, a criterion on a SMOS-retrieved pseudo-dielectric constant (ACARD parameter, defined in **?**)) was applied to discard SMOS measurements affected by sea ice (discarded when $ACARD < 45$). The ~~error~~ uncertainty of SMOS SSS "A" was derived from the propagation of the ~~error~~ uncertainty on individual SMOS ESA L2 SSS pixel during 7 days. The ~~error increases strongly~~ uncertainty strongly increases in the vicinity of sea ice ~~.~~(Fig. 5, b). For this reason, in the following study, above 75°N, all pixels with an SSS weekly ~~error larger that~~ uncertainty larger than 0.8 were not considered. South of 75°N, a higher threshold was used (1.5) allowing to maintain some measurements closer to fresh river water from the Lena and the Khatanga Rivers near the coast. In this area, the χ^2 may increase due to the strong heterogeneity of SSS within SMOS multi-angular brightness temperatures footprints, and the number of measurements is low due to the presence of the coast and islands even without sea ice. ~~A theoretical error~~ The theoretical uncertainty of SMOS SSS "A" field is below 0.5 in the center of the Laptev Sea and up to 2 and higher close to the coastline and MIZ.

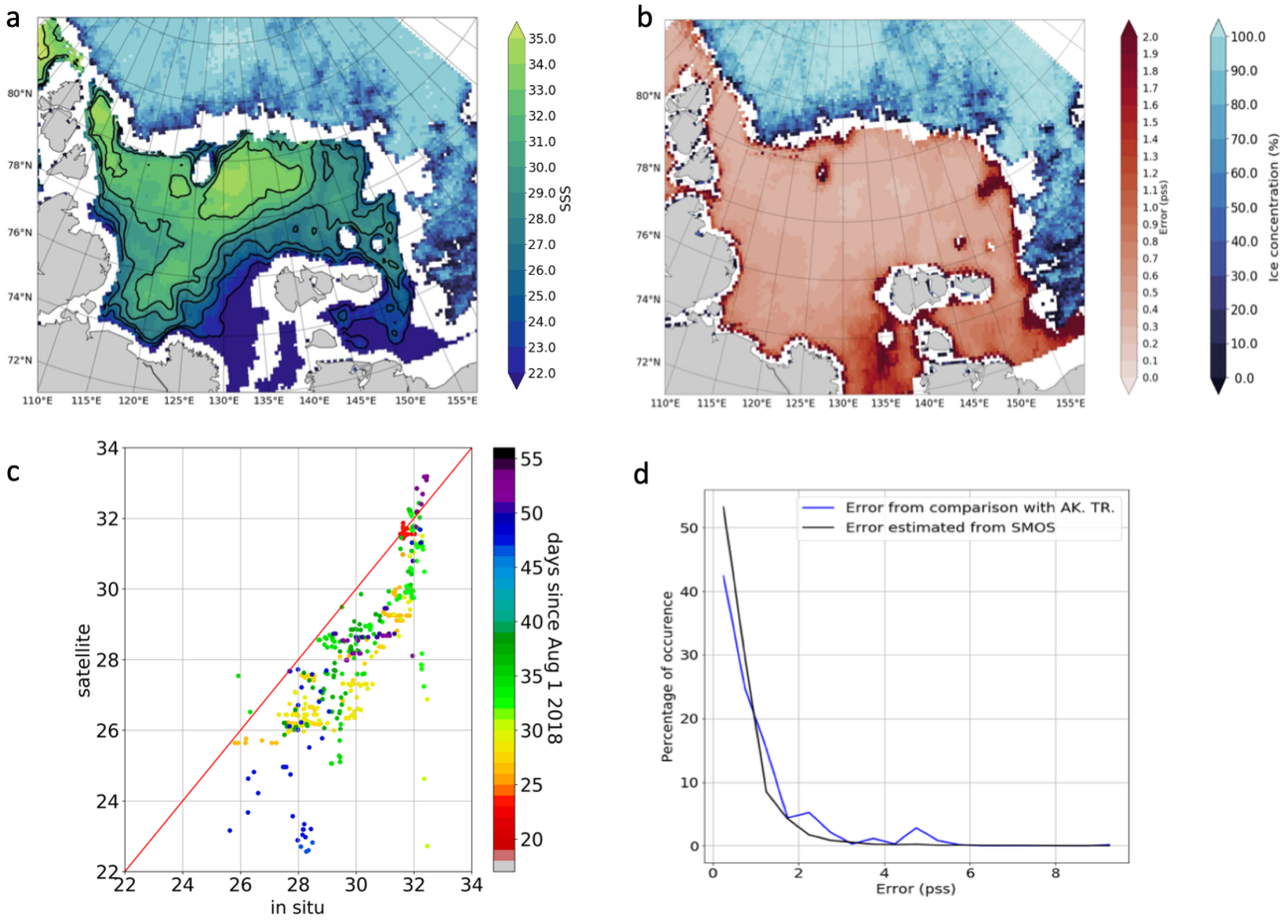

Figure 5. Sea surface salinity validation: example of SMOS SSS "A" for September 13, 2018 (a), ~~computed error estimates for this day~~ and associated uncertainties (b), ~~comparison~~ scatter plot of co-located SSS and ~~in situ~~ *in situ* data in the upper 6.5 m (c) and statistical distribution of provided SMOS L2 ~~error~~ uncertainties and measured absolute difference from comparison with ~~in situ~~ *in situ* data (d). Sea ice concentration from AMSR2 is indicated with blue shading on the upper panels

2.2.4 Validation of SMOS "A" SSS

In this section, we compared the SMOS SSS "A" relative to ~~in situ~~ *in situ* measurements. Figure 5 presents the SMOS SSS "A" on September 13, 2018, the same day as the DMI SST in Fig.4. We carried a co-location of SMOS SSS "A" and ~~in situ~~ *in situ* measurements of salinity in the upper 6.5 m layer in a following manner: the averaging of the TSG salinity was done over one hour period (equal to $\sim$ 15 km distance, contrary to DMI SST validation) in order to be closer to SMOS SSS "A" spatial resolution. We used 985 collocated points.

Comparison between the ~~in situ~~ *in situ* practical salinity and SMOS SSS "A" shows a very good agreement, not yet demon-

strated before by any other salinity product in the Laptev Sea. The correlation coefficient is 0.86 with a RMS = 0.86. The mean difference is 2.06~~.~~, SMOS SSS being lower than *in situ* surface salinity. This underestimate could be related to the presence of land in the very wide SMOS field of view as observed at lower latitudes by **?**, and this difference appears to be, at first order, systematic (Fig.5, c). In what follows, we subtract this mean difference from the entire SMOS SSS dataset. The standard deviation of SMOS SSS with respect to ~~in situ~~ *in situ* SSS does not vary with the depth of the ~~in situ~~ *in situ* salinity measurements above 6.5 m, either because ~~in situ~~ *in situ* salinity was homogeneous vertically or because comparisons were too noisy to detect ~~this~~ these small variations (not shown). Although SMOS SSS "A" shows a good agreement most of the time, some larger ~~errors~~ uncertainties occur close to the sea ice margin or when pixels are contaminated by small ice pattern not detected by AMSR2 sea ice concentration algorithm (as at 80°N 125°E in Fig. 5, a).

Comparison between SMOS ~~retrieved error~~ uncertainties and error based on comparison with ~~in situ~~ *in situ* salinity measurements is presented in Fig. 5 (d). The percentage of occurrence is computed in salinity classes with a size of 0.5 that starts at 0. It shows a rather good agreement between the distribution of SMOS SSS "A" ~~error~~ uncertainties estimated from retrieval process and the distribution of error obtained from comparison with ~~in situ~~ *in situ* salinity measurements. ~~This~~ The uncertainties are in 85% of cases less than 1.2, which is relatively small compared to spatial gradients shown on Fig.5, a. These results allow us to use the SMOS SSS "A" error with confidence ~~in our further~~ for this analysis. Using error filtering, the points too close to the ice edge were excluded.

2.2.5 Sea ice concentration and ice masks

Sea ice masks were obtained from AMSR2 sea ice concentrations products provided by the University of Bremen (**?**): they are weather-independent, thus, continuous for the whole period. The highest available spatial resolution is 3.125 km. The AMSR2 ice masks were used in addition to the masks provided with every satellite product discussed (DMI SST, SMOS SSS "A", ASCAT (Advanced SCATterometer) winds L3 (see its description below)). A continuous erroneous presence of ice along the Siberian coast was observed and had to be filtered: images in optical band and the ice charts from the Arctic and Antarctic Research Institute (AARI) were used as a reference (can be found at http://www.aari.ru/odata/_d0004.php). As it was detailed above, an additional filtering was applied to SMOS SSS "A" as the L-Band measurements are sensitive to ice thicknesses less than 50 cm contrary to AMSR2 measurements.

The sea ice opening starts relatively late in the Laptev Sea: a coastal polynya appeared in the southern-central part of the Laptev Sea at the beginning of June in 2018 and by the beginning of August, the sea was ice-free only south of 79°N. The Laptev Sea was completely covered by the beginning of November in 2018. For this study, we define the sea ice edge with the position of 1% sea ice concentration and MIZ as 0-30%.

2.2.6 Wind speed

To investigate the wind speed pattern, we use ASCAT scatterometer daily C-2015 L3 data produced by Remote Sensing Systems. Data are available at www.remss.com.

2.3 Reanalysis data

Reanalysis data are used to include some additional parameters not available from satellite and ~~in situ~~ *in situ* data. Atmospheric forcing fields: sea level pressure, SLP, and air temperature, are obtained from the ERA5 reanalysis (**?**). The latest reanalysis of ERA5 still has relatively crude spatial grid of 0.5°for the SLP and 0.25°for air temperature.

2.4 Ekman transport

To investigate the role of the wind forcing, we compute mean monthly wind fields and the Ekman transport for August and September 2018. Horizontal Ekman transport, m^2/s, is calculated as:

$$\begin{aligned} u_{Ekm} &= \frac{\tau_v}{\rho_w * f} \\ v_{Ekm} &= -\frac{\tau_u}{\rho_w * f} \end{aligned} \tag{1}$$

where u_{ekm} and v_{ekm} are horizontal components of the Ekman transport, τ is a wind stress, calculated from ASCAT winds (u_{wind}, v_{wind}) using ERA5 air density ρ_{air}: $\tau_u = C_D * (u_{wind}) * u_{wind} * \rho_{air}$; ρ_w is a surface density, calculated from SST and SSS with TEOS-2010 (**?**); C_D is surface drag coefficient calculated from wind speed according to **?**: for the wind speed U_w below 10 m/s $u_{star} = 0.051 * U_w - 0.14$ and for the stronger winds: $u_{star} = 0.051 * (U_w - 8) + 0.27$; f is the Coriolis parameter.

~~The Ekman pumping (upwelling and downwelling) was computed as:~~

$$w_{ekm} = \frac{1}{\rho_w * f}\left(\frac{d\tau_v}{dx} - \frac{d\tau_u}{dy}\right) + \frac{\beta * \tau_u}{\rho_w * f^2}$$

~~where w_{ekm} is the Ekman vertical velocity and β is the y-derivative of the Coriolis parameter.~~

3 Results

3.1 Overview of SST and SSS in the Laptev and East-Siberian Seas in August-September 2018

The mean SST during the 2 summer months is 2.18°C in the Laptev Sea (between the Severnaya Zemlya Archipelago and the New Siberian Islands), and 1.13 °C in the ~~studied~~ part of the East-Siberian Sea investigated (Fig. 6). The highest temperatures (above 6°C, up to 9°C) were observed close to the Lena River delta in the Yanskiy Bay and in the Olenekskiy Bay in front of the Khatanga River. A warm water pool associated with the river plume between 125°E and 135 °E progressively propagates ~~northeast~~ north-eastward and warms up this part of the sea: 0°C isotherm at 140°E meridian is situated 100 km northward compared to its position at 120°E. The studied part of ~~the~~ western East-Siberian Sea was not completely ice-free in August-September 2018. Negative temperatures are observed near the ice edge at a distance of 50-100 km of the ice edge almost

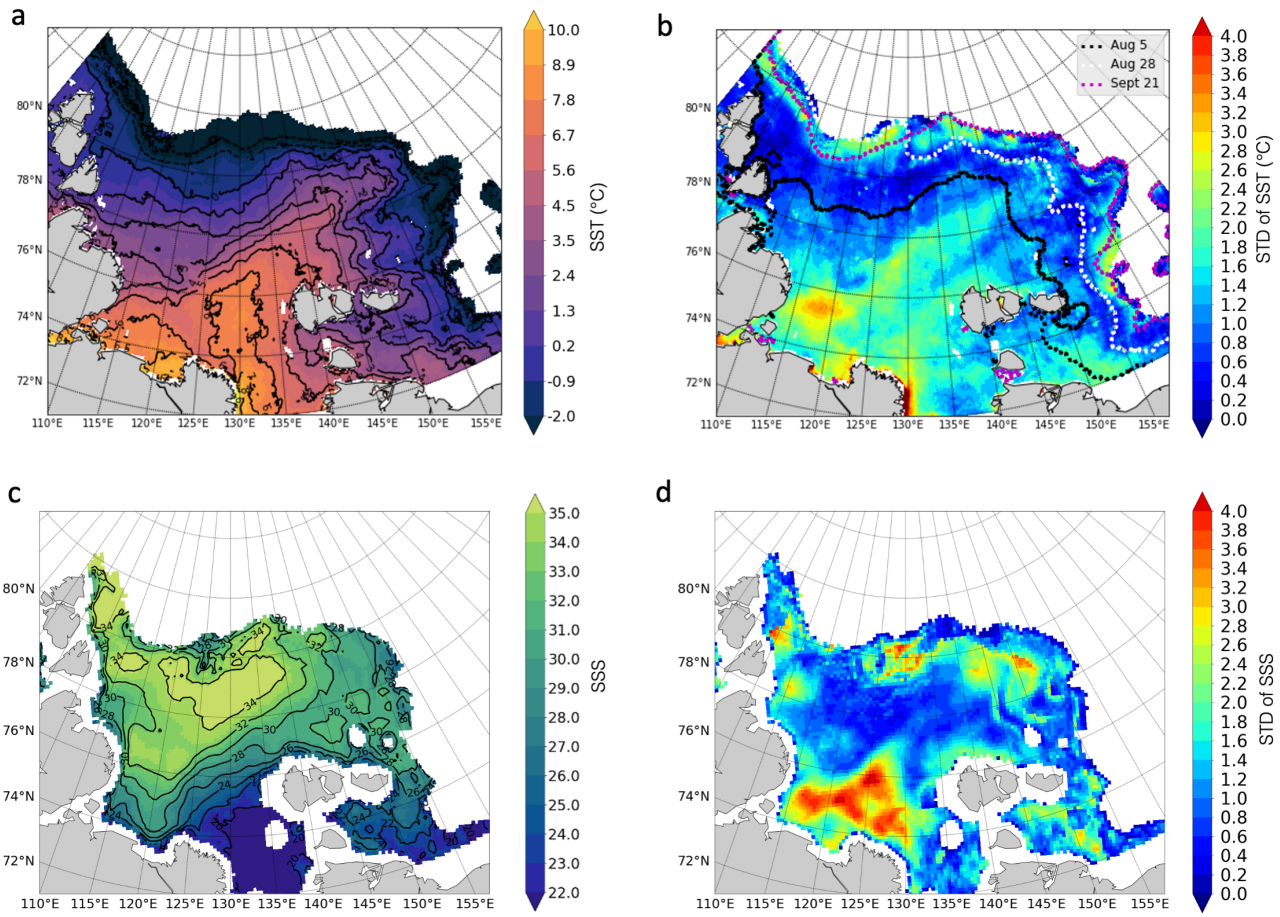

Figure 6. Mean DMI SST (a) with its STD (b) and mean SMOS SSS (c) with its STD (d) for August-September 2018. The dotted lines in Figure (b) show the position of sea ice edge at different moments of time before and during the ARKTIKA-2018 cruise

everywhere, except for a small area at 80°N 160°E, where warm river water meets the sea ice ~~and~~ with no open water with negative temperatures~~is seen~~. The strongest gradients are observed along the sea ice edge and the river water plume (up to 0.05° C/km~~, gradient~~). Standard deviation of SST in Fig.6 is the largest in the Olenekskiy Bay (over 2.5°C), along the coastline close to the Khatanga estuary (2.5-3°C), the Lena River delta (about 4°C) and in marginal ice zone (mostly over 1.5°C). The remarkable variation of SST in the central part of the Laptev Sea should be associated with the thermal fronts (largest SST gradients) displacement.

The averaged SSS is 28.75 (with uncertainty of 0.10) in the Laptev Sea and 27.74 ~~in the studied part of the~~ (with uncertainty of 0.20) in the western East-Siberian Sea (Fig. 6). The spatial distribution of mean salinity for August-September 2018 ~~has several characteristic features. The~~ shows the freshest water (salinity below 20) ~~are observed~~ within the river plume northeast of

the Lena River delta and within the southern part of the East-Siberian Sea. Water with salinity below 28 reach the sea ice edge in the northeast Laptev Sea. Additional fresher water from the Kara Sea enters via the Vilkitskiy and Shokalskiy straits in the west (salinity of 28-30) and is also observed along the sea ice edge, ~~so~~ where it could be associated with ice melting. The most saline water (salinity above 34) is located in the central part of the Laptev Sea near 78-80°N 120-140°E, and in the northwest, along the Severnaya Zemlya Archipelago. As also observed in ~~the SST, the~~ SST, SSS in the Olenekskiy Bay is highly variable, which can be explained by the variation of the freshwater discharge during the 2 months. Nevertheless, large SSS variability is also observed all along the sea ice edge: at 78-80°N in the north and northwest and at the boundary between the Laptev and East-Siberian Seas. This large variability can be explained in two ways: physical (haline fronts related to sea ice melting) and instrumental (remaining ice contaminated pixels, lower sensitivity of L-band in cold water). At 78-80°N 125°E, free-floating patches of broken ice detached from compact sea ice edge are observed during several weeks in August-September 2018. Random pieces of broken sea ice are not always recognized by ice-mask filters, so can artificially increase ~~the~~ SSS variability. At the same time, this is the area where river water ~~meet~~ encounters sea ice, which induces natural variability.

3.2 Observed surface water masses of the Laptev Sea and their transformation

To generalise our understanding of vertical structure of the studied area, we use the classical TS-analysis, first based on CTD measurements~~only~~. Fig. 7 shows the temperature-salinity distributions in the upper 200 m, ~~where the color of marker indicates~~ coloured as a function of depth. The most prominent feature on the diagram is the transformed Atlantic Water mass with salinity close to 34.5-35, temperatures from -0.5 to 2.5 °C lying at a depth of 100-200 m. The water mass overlying the Atlantic Water (between 50 and 100 m depth) is the lower halocline water, described by **?** as having salinity in a range of salinity 33-34.5, and negative temperatures starting from the lowest values presented in Fig. 7, -1.7 to 2.5°C. The surface water observed in the upper 50 metres is in general ~~the~~ less saline (salinity below 34), but ~~one~~ we can clearly observe two separate branches with negative and positive temperatures. The two upper-layer branches are (1) warmer ($[-1;6]°C$) and low-saline (below 34) surface water of the ice-free Laptev Sea and (2) colder ($[-2;0]°C$) and low-saline waters of the ice-covered East-Siberian Sea. The latter correspond to the measurements from the sections 7 and 8 eastward of 150°E.

It should be remembered that a T-S diagram based only on CTD measurements does not provide an instantaneous view on the ocean state, but is a collection of conditions encountered in different regions at different ~~moments of time~~ times (from the end of August to the end of September 2018). During the summer months, the surface water of the Arctic Ocean quickly ~~changes its characteristics~~evolves, and the synoptic satellite data provide an additional information to the point-wise ~~in situ~~ *in situ* measurements.

Using DMI SST and SMOS SSS weekly estimates, we plotted T-S diagrams similar to ~~that on~~ the one in Fig.7, but ~~for~~ only for surface satellite measurements for several reference days: Aug 1, Aug 15, Aug 30, Sept 4, Sept 13, and Sept 30, 2018 (Fig.8). On the lower row, we present all ~~in situ~~ *in situ* measurements in the upper 6.5 m and the differences between satellite-derived sea surface temperature and salinity ~~of discussed days.It is observed that the DMI SST is rising~~ for the selected day. The range of variation in SSS and SST values covered by the satellite measurements (first row of Fig.8) is an order of magnitude wider than the one covered by *in situ* measurements (Fig.8, first column, bottom row). The difference in T-S diagram

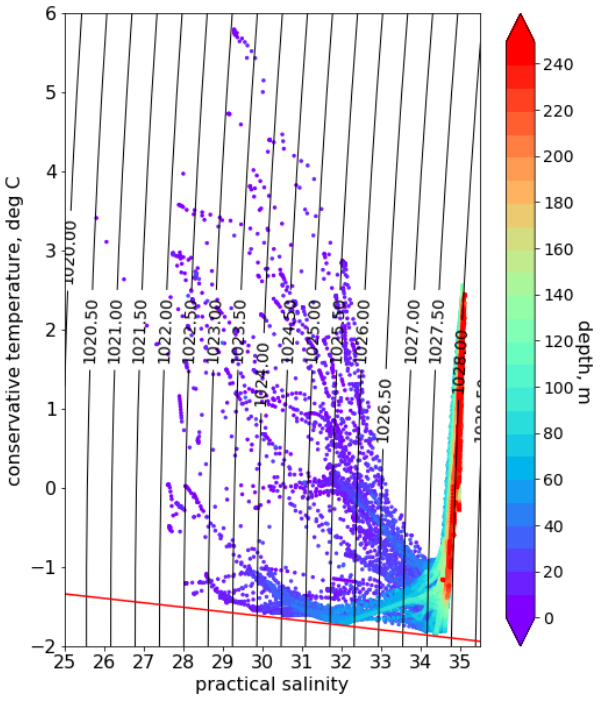

Figure 7. T-S diagram based on the CTD data in the upper 250 m, colour-coded by depth. ~~Depth of each measurement is shown with color. Red~~ The red line shows the freezing ~~point~~line.

covered by each type of measurement cannot be explained the errors of satellite measurements (RMS difference with respect to *in situ* measurements of 0.77°C and 0.8 in temperature and salinity, respectively), nor by the uncertainties associated with each satellite product (Fig.4, b and Fig.5, b). It primarily reflects the much better spatio-temporal monitoring of different water masses by satellite measurements. The DMI SST rises only up to the end of August with the maximum temperatures from 8 to 11.5°C ~~for~~ in some cases, and then decreases to 4.5°C by the end of September. The temperature is changing by 0.5 - 1°C per week (while increasing and decreasing).

Based on the Fig. 8 visual analysis, we propose to identify 6 surface water masses in the Laptev and East-Siberian Seas (Tab.1) ~~.~~to follow the transformation of surface waters during 2 summer months. The number and the limits of water masses were arbitrarily chosen based on the temperature-salinity scatter plot for September 4, 2018, as this day allow to separate the cores of surface waters into groups in the best way based on the density of points. The temperature and salinity ranges of variation of each class are also well above the T and S uncertainties.

The main surface water masses are warm and fresh (WF) river water and cold and saline (CS) open sea water. All other water masses show either different stages of transformation of these two water masses, or are advected from other regions. It should be noted that satellite-derived data have a larger range of temperature and salinity than the near-surface (upper 6.5 m) ~~in situ~~ *in situ* measurements, which ~~makes~~ enables this detailed classification~~possible~~. The locations of the different water masses for ~~selected~~ specific days are shown in Fig.9 together with the percentage distribution of water masses ~~in percentage~~ (the whole studied area is 100%, and sea ice occupies some part of it).

On August 1, the sea ice still covers more than 80% of the studied area and extends on average to 78°N in the Laptev Sea, while the East-Siberian Sea is almost completely covered by ice. Warm and Fresh (WF) river water is well observable in the ~~south~~ southern parts between 74 and 76°N. It occupies almost the same amount of surface as the Cold and Saline sea Water (CS), the rest of the open area is occupied by a transformed river water (Warm and Medium Salinity, WMS, Cold and Medium Salinity, CMS), that already formed a recognisable river plume front: its signature is continuous from 115°E to 150°E up to the northern position of sea ice edge.

During the next two weeks the ice cover retreats, and a Cold and Fresh Water (CF) mass appears in the south-west East-Siberian Sea. The amount of this Water increased progressively in this area during the remaining period. We suggest that this water mass represents the river water trapped under the ice and then exposed (see results of geochemical analysis below in Section 3.3.4).

On the 15th of August, ~~one can notice as well~~ a water mass CMS ~~appearing close to~~ also appears close to the Vilkitskiy Strait. It is less pronounced by the end of August, but a thin stream of cooled and transformed river water from the Kara Sea descends along the Taimyr peninsula in September. The Lena River water mixing and cooling happens as well close to the sea ice edge in the north-east Kara Sea. ~~All in all~~As a whole, the surface occupied by this water mass is steadily growing during the observed period ~~, and is~~ to reach nearly 10% of the surface by the end of September. We suggest that water mass CMS is a transformed version of water mass CF.

The end of August is warmer as seen in Fig. 9 with the amount of saline water with temperatures above $3°C$ (water mass WS, Warm and Saline) occupying the central and the western part of the Laptev Sea (almost 10% of the studied area). This water mass ~~is disappearing~~ disappears by the end of September with ~~a~~ the seasonal decrease of temperature.

By September 13, the SST and SSS variability diminishes. The water mass CF in the north-east Laptev Sea consisting of cold fresh water becomes saltier (transforms into the water mass CMS). The freshwater cools south of the New Siberian island and by September 25 occupies all the ice-free area. The river plumes signature ~~is shifted~~ shifts as well to the New Siberian island as well (Fig. 9). Cold and saline water dominates the surface of the Laptev Sea. Finally, by September 25, the T-S diagram shows that most of the SSS/SST points lay between 25 and 35 and -1°C and 4°C, with a main core within a salinity range 25-35 and temperature between -1 to 1°C, and the second one within the salinity range 22.5-30 and temperature of 3-4°C. The Laptev and the East-Siberian Seas start then to refreeze, the most rapidly in the areas with cold and fresh river water.

3.3 Freshwater variability in the Laptev Sea

To evaluate the distribution of freshwater input in the Laptev Sea in August-September 2018, we consider ~~virtual~~ zonal and meridional transects along 78°N and 126°E, respectively, and plot the temporal evolution of DMI SST, SMOS SSS "A", wind

Table 1. The temperature and salinity of six defined surface water masses of the Laptev Sea using satellite data (see the text for the explanation of water masses names)

Water mass	WF	WMS	CF	CMS	WS	CS
T	$> 3°C$	$> 3°C$	$< 3°C$	$< 3°C$	$> 3°C$	$< 3°C$
S	< 25	$25 - 29$	< 25	$25 - 29$	> 29	> 29

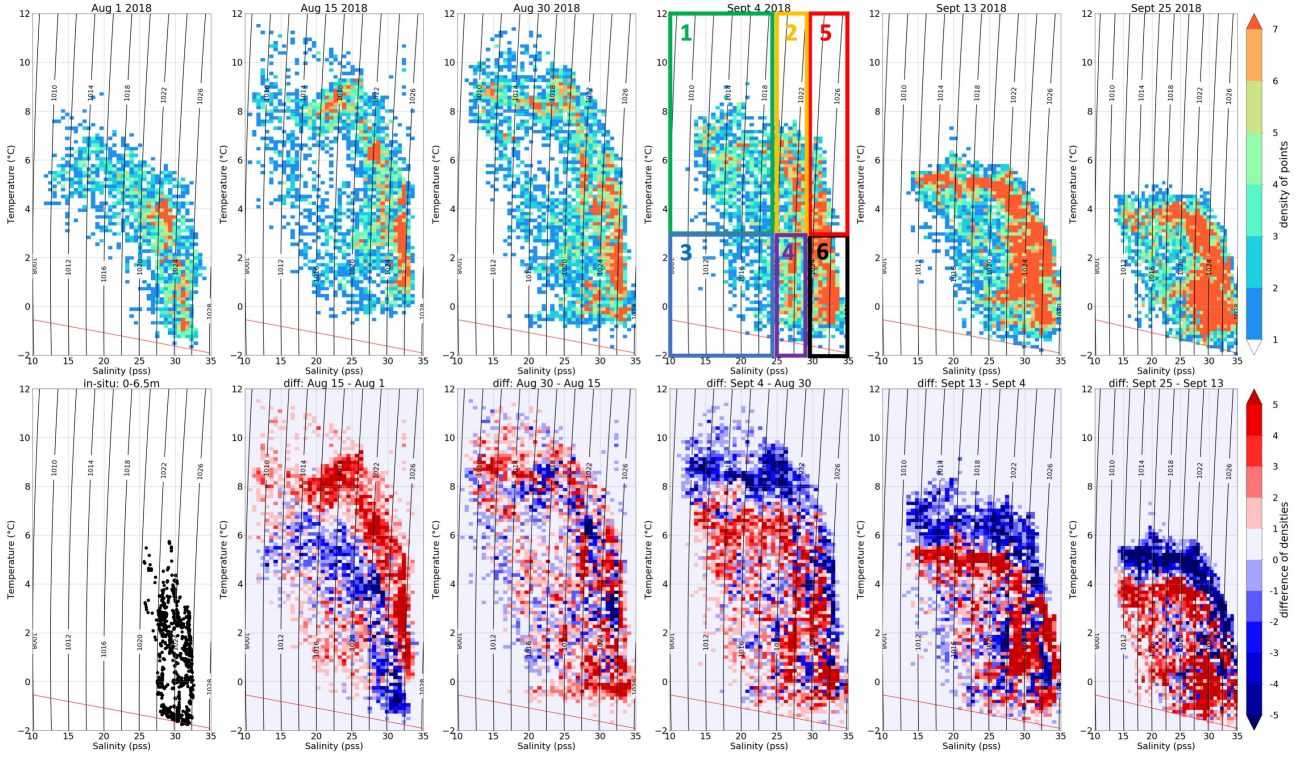

Figure 8. Temporal evolution of surface water masses in August-September 2018 for the following reference days (upper row): Aug 1, Aug 15, Aug 30, Sept 4, Sept 13, and Sept 30, 2018. ~~Color~~ colour represents the density of points (number of observations with this temperature and salinity). ~~Red~~ The red line shows the freezing point temperature for different salinity. The boxes show the cores of 6 water masses described in text: 1 - WF, 2 - WMS, 3 - CF, 4 - CMS, 5 - WS, 6 - CS. Lower row: column 1, the T-S diagram based on CTD measurements in the upper 6.5 m only, and from column 2 to 6, the differences (in density points) between the reference days.

speed and SLP in Hovmöller diagrams. The freshwater can be defined by comparison to the saline “marine water” (typically, 34.80 as in **?** or 34.92, as in **?**). As a 0-salinity river water quickly mixes with a saltier marine water, in reality the "freshwater" is more "brackish" than "fresh". Nevertheless, for simplicity assuming a river plume front at the 29 isohaline, the “freshwater” corresponds to all water masses with the salinity lower than 29, as we referred to it in section 3.2.

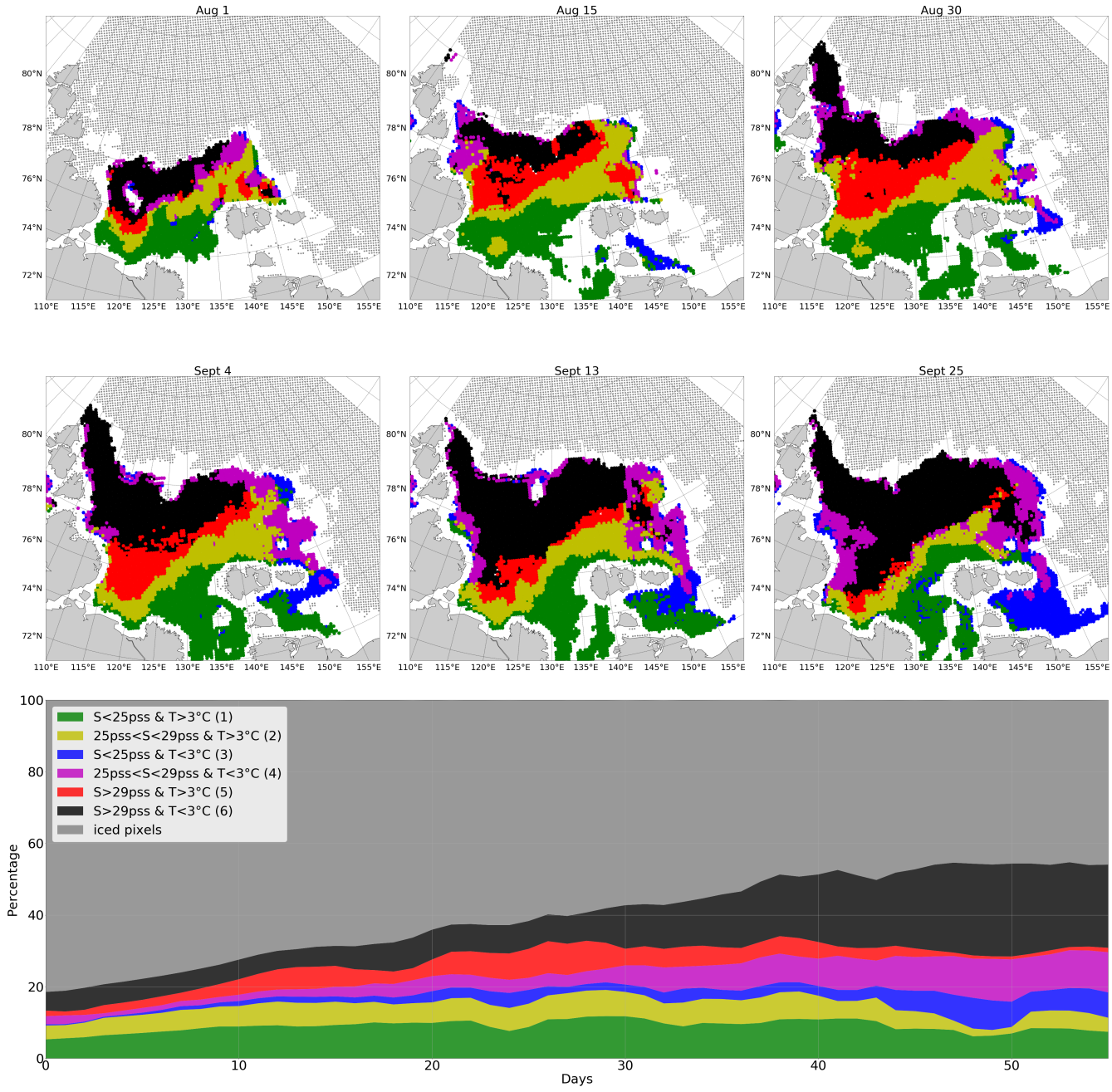

Figure 9. Spatial distribution of surface water masses in August-September 2018: upper row - Aug 1, Aug 15, Aug 30; ~~lower~~ middle row - Sept 4, Sept 13, Sept 30. Sea ice cover from AMSR2 is plotted as dashed area. The lowest panel show temporal evolution of surfaces occupied by each water mass or sea ice cover in the Laptev Sea (in % of the Laptev Sea surface).

3.3.1 Water from the Lena River plume

The zonal transect helps to investigate the mean stream position of the river plume away from the coast, in the central part of the Laptev Sea with more complex topography (Fig. 10). This virtual section does not correspond to any real CTD-section, apart from some ~~extracts of TGS profile~~ TGS profiles following the ship's route (see the position of virtual section on the SST and SSS maps in Fig.10, f-g). In the western part (up to 130 °E), the transect is located roughly above the continental slope and then over the shelf (Fig.10, e). The river water displacement roughly follows that of sea ice edge in the east and is bounded by the shelf break in the west. Overall, temperatures are higher in August than in September: a warm pool with SST over 6 °C is observed during the first 30 days at 78°N, 130-147 °E, with highest temperatures on August 26. These coordinates define the position of the river plume at 78°N latitude, as can be clearly seen in the salinity values varying in a range of 27-30~~there~~. Relatively strong daily winds (10-12 m/s) observed during the first 10 days of September were associated with a series of cyclones, which strongly impacted the surface layer: the median temperature over the zonal transect decreased from 3°C to almost 0°C, and salinity increased by 1. As the amount of incoming solar radiation diminishes in September, the maximum SST values did not exceed 3°C anymore. Nevertheless, at the end of September, a new freshwater patch was observed at 140°E (less visible in SST field) indicating that the "upstream" surface mixed layer (in the southern part of the Laptev Sea) contained a sufficient amount of freshwater to restore its previous state after a mixing event induced by the wind. Another possible explanation is that a small peak observed in the Lena River discharge in the first days of September (Fig.3) ~~helped to introduce~~ introduced an additional portion of freshwater that reached 78°N several weeks later.

3.3.2 Water from the Kara Sea

The zonal transect allows to see not only the Lena River plume, but as well the Kara water intrusions in the west. The selected zonal transect at 78°N is partly lying ~~above~~ in the Vilkitskiy Strait connecting the Kara and the Laptev Seas. Being a reservoir for two other great Siberian Rivers, the Ob' and the Yenisei, the Kara Sea has a low salinity compared to the central Arctic Basin (**?**). In the absence of significant river sources on the Severnaya Zemlya Archipelago, we considered that the freshwater input close to the Vilkitskiy and the Shokalsky Straits arrived from the Kara Sea.

We observe the freshwater arriving from the Kara Sea at 110-115°E with typical values of 25-28 during the first 20 days of August and at the end of September (Fig.10, b). It is noteworthy that the SST fields do not indicate so clearly the presence of these intrusions~~so clearly~~. This suggests that fresh and warm water of the Ob' and Yenisei rivers arriving to the Laptev Sea have already lost a significant part of their heat content ~~via exchange with~~ to the atmosphere, but that the freshwater layer is not completely mixed with the surrounding sea environment.

In Fig. 11, the CTD data justify that the amount of freshwater arriving from the Kara Sea ~~via~~ through the Vilkitskiy Strait is significantly greater than freshwater arriving via the narrow and rather shallow (250 m) Shokalskiy Strait between the Bolshevik and the October Revolution Islands or north of the Severnaya Zemlya Archipelago at the traverse near the Arkticheskiy Cape across the continental slope. The temperature of the surface layer is increasing between 0°C ~~to~~ and 3.5°C from ~~the North to the South. The salinity sections indicate the~~ north to south. Salinity sections indicate freshwater with salinity above 29 only

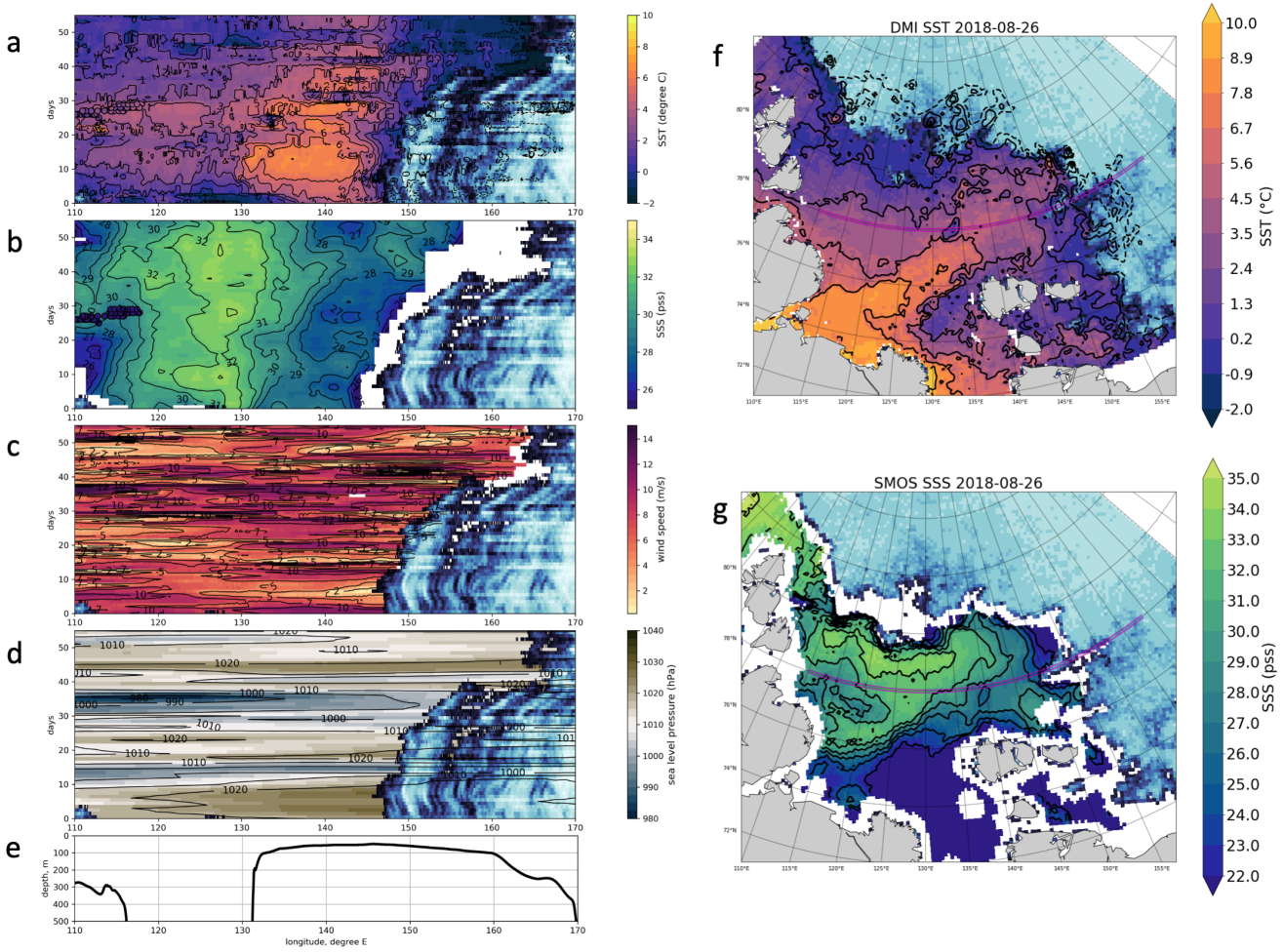

Figure 10. Hovmöller diagram of DMI SST (a), SMOS SSS "A" (b), ASCAT wind speed (c), and ERA5 sea level pressure (d) for the zonal transect at 78°N. Small coloured circles ~~at~~ on SST and SSS diagrams (a, b) show ~~in situ~~ *in situ* measurements of temperature and salinity (first CTD or TSG at 6.5 m). Sea ice concentration (AMSR2) is indicated with a blue ~~color~~colour, see Fig.5 for the ~~color~~ colour scale. The bathymetry along the virtual transect (e) is extracted from "1 Arc-Minute Global Relief Model" (**?**). The position of a virtual transect is shown ~~at~~ on DMI SST ~~SMI~~ and SMOS SSS "A" maps for August 26, 2018 (f, g) with magenta lines.

in the Shokalskiy and the Vilkitskiy straits, which suggests very little advection of the Kara-origin freshwater via the north. From the buoyancy cross-sections, ~~one can~~ we find that the strongest stratification is at 5-20 m depth, which corresponds to the 1024-1025 kg/m^3 isopycnals ~~position~~depths. This result argues against a definition of fresh-water content by the 1027.35 kg/m^3 isopycnal of **?**, as the surface salinity and temperature in the Siberian shelf seas are lower than in other regions.

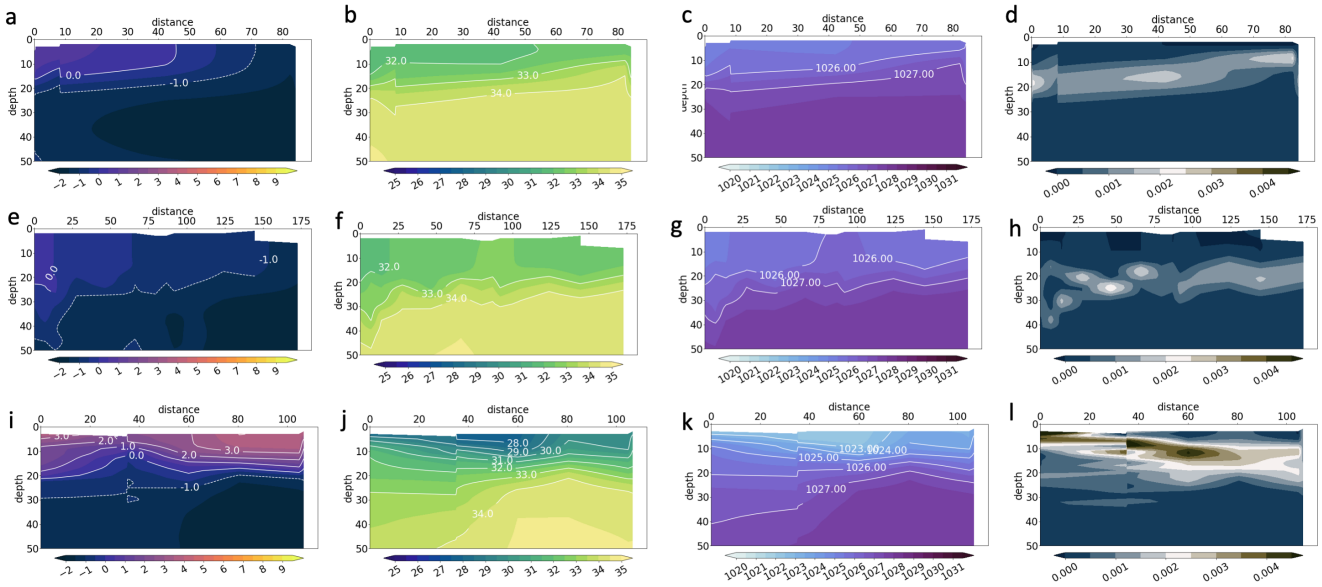

Figure 11. Temperature, °C, (left, first column), salinity, (second column), water density, kg/m^3 (third column) and buoyancy frequency, s^{-1}, (right, ~~forth~~ fourth column) obtained from CTD measurements in the upper 50 m for section 1 northward of Arkticheskiy Cape (upper row), section 10 across the Shokalskiy Strait (second row), and section 4 across the Vilkitskiy Strait (lower row). See Fig.1 for the section's positions. The zero km is always placed at the southern point of each section

3.3.3 Meridional transect

The meridional transect along 126°E (Fig. 12) partly corresponds to the standard oceanographic section 5 carried out during ARKTIKA-2018 expedition on September 1-4, 2018 (Fig.13). This transect helps to understand the northward propagation of the river plume and to evaluate the freshwater content using ~~in situ~~ *in situ* data. The highest SST observed along 126°E longitude is 8°C in August (please note, that a small cold temperature intrusion on days 22-26 probably corresponds to an error in DMI SST product due to a cyclone passage and thus, either bad cloud masking or strong winds. This is an assumption reinforced when comparing DMI SST to SST AMSR2 microwave data (not shown here). More information on the SST corrections in the Arctic can be found in the work of **?**).

The warmest (5-9°C) and freshest (salinity of 20-30) water of river plume occupies the area between 74-77°N in August and progressively retreats in September: SST and SSS gradients become wider and less pronounced, temperature decreases to 3-4 degrees. High wind speed (10-12 m/s) associated with an atmospheric cyclone passage during the first two weeks of September is found both on the meridional and the zonal Hovmöller diagrams and might explain this widening of the surface thermal and haline frontal area. Nevertheless, a point-wise cross-correlation between the time-series of wind speed and temperature or wind speed and salinity ~~in a point with random coordinates~~ does not give statistically significant results: both correlation coefficients are below 0.2 at any time lag (0-10 days). Better correlation is observed with sea level pressure (up to 0.6 at some points), but

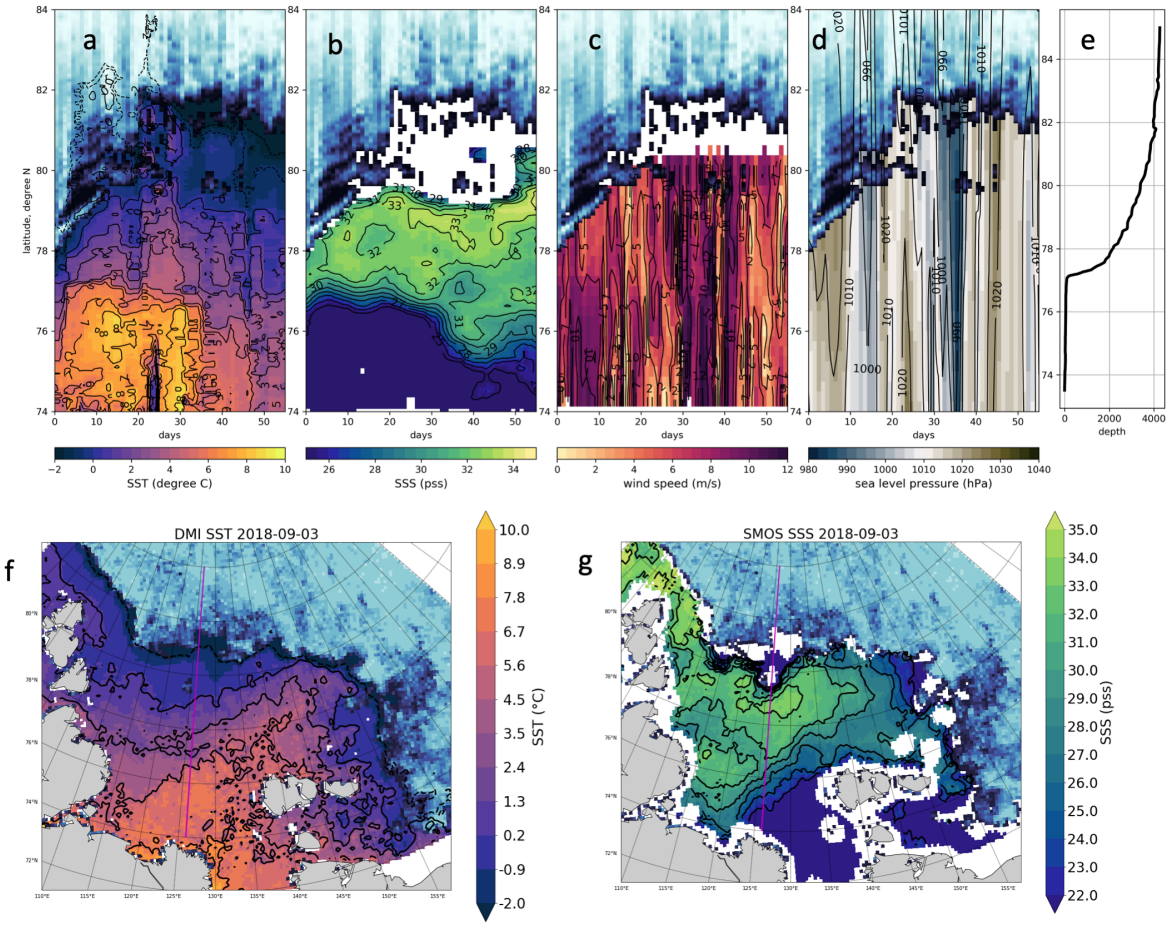

Figure 12. Hovmöller diagram of DMI SST (a), SMOS SSS "A" (b), ASCAT wind speed (c) and ERA5 SLP (d) for the virtual meridional transect at 126°E. Sea ice concentration (AMSR2) is indicated with a blue ~~color~~colour, see Fig.5 for the ~~color~~ colour scale. The bathymetry along the transect (e) is extracted from "1 Arc-Minute Global Relief Model" (**?**. The position of a virtual transect is shown on SST SMI and SMOS SSS "A" maps for August 26, 2018 (f, g) with magenta lines.

over the 56 days ~~of the studied period~~ investigated it is not statistically representative as only two ~~passages of cyclone~~ passing cyclones were observed.

The oceanographic sections allow to estimate a thickness of the freshwater layer and how far the river water propagates under the ice. Section 5 provides ~~a~~ complementary information to the meridional Hovmöller diagram (Fig.13, upper row) as it was done along the same 126°E parallel from 76 to 81.4° N on September 1-4 2018. This date corresponds to the passage of several cyclones over the Laptev Sea, which, in turn, displaced the river front to the south, unfortunately, almost away from this oceanographic section. Nevertheless, at 76-78° N (first 200 km of the section), low salinity between 29-33 was still observed in the upper 25 meters. A thin upper layer with positive temperatures has the same thickness, but extends further northward,

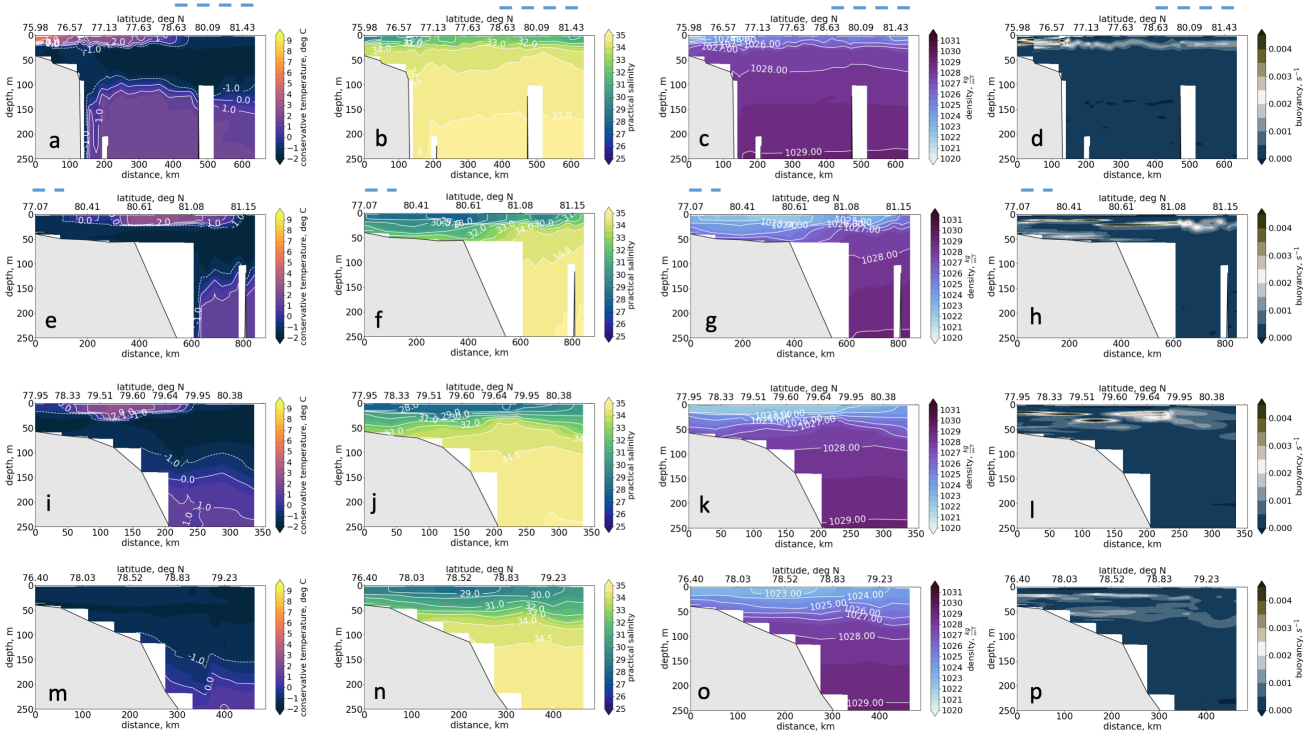

Figure 13. Conservative temperature (left, first column), practical salinity (second column), density (third column) and Brünt-Vaisälä frequency (right, last column) in the upper 250 m along oceanographic section 5 (a-d); section 6 (e-h); section 8 (i-l); and section 7 (m-p). See Fig.1 for the section positions. The zero km is always placed at the southern point of each section. The dashed blue line indicates the MIZ for sections 5~~and~~ , 6 and 8 (the rest is ice-free area); the full line indicated that the section 7 ~~and 8 were~~ was done under the ice~~in MIZ~~.

up to 79° N. In the ~~north~~ northern part of the section, under the ice, the temperatures are below 0°C and salinity is rather low, below 32. The low salinity under the ice suggests that the ~~residuals~~ remnants of the river water arrived in this area earlier. If the river water were propagating under the ice when the Laptev Sea was not yet completely open, we should assume their further mixing with sea water when the sea started to open in its central part (mixed water with salinity between 30 and 32 and still positive temperatures). The heat exchange with the sea ice might be more effective than with the atmosphere, so under the ice the temperatures are negative, and the warm river water signal is not observed anymore, contrary to salinity. At the same time, it depends on thermal conductivity in the ice, and its initial temperature profile, so this question needs ~~a special~~ further attention.

Overall, the first 150 km over the shelf, where the warmest and freshest water were observed, are characterized by the strongest stratification in the upper 25 m layer. This is the depth of a stable stratification for the whole section, though stratification is less pronounced in the deeper part of the sea than over the shelf. Below the pycnocline, ~~one can~~ we observe cold (with negative temperatures) and saline (salinity between 33 and 34.5) water mass. The warm (T above 0°C, following **?**) and

saline (S above 34) Atlantic Water spreading along the continental shelf is best identified in temperature vertical profiles at 100-120 m depth, but is also detected by the instability signal (right column in Fig. 13). The propagation of the Atlantic Water is beyond the scope of this paper, and though Atlantic Water is observed in all oceanographic sections presented below, it won't be discussed furthermore.

When considering other meridional sections (~~section~~ 6, 8, and 7 according to their positions~~from the west to the east), one can~~), we follow the eastward propagation of the river water away from the Lena River delta. Section 6 started on September 5 in the vicinity of the marginal ice zone in the deep North-Eastern part of the Laptev Sea and ended in the ice-covered part of the East-Siberian Sea over the shelf on September 9. This section is not exactly perpendicular to the continental slope, so we ~~can not~~ cannot estimate the width of the river water plume, but overall the thickness of the upper layer is similar (20-30 m) to that observed with section 5 in the deep part of the section. The ~~water~~ waters over the shallowest part (depth smaller than 60 m) were observed under the ice, as is clearly seen in the temperature signal that is negative even close to the surface. At the same time, the main freshwater core with the highest temperature is observed above the shelf break. The second core is observed in the northern part of the section, with lower salinity than in the north of section 5. The mixing over the shelf was effective enough to stretch the isopycnals between the bottom and the surface. Nevertheless, the depth of the maximum stratification is close to 20 metres as for the shallow part of the section 5. Over the edge of the continental slope, the maximum Brünt-Väisälä frequency moved deeper to 25 m, and over the deep-water part to 30 m depth.

Section 8 ~~was~~ started on September 15 in MIZ over the deep part of the East-Siberian Sea and finished by September 17 in the ice-free area over the shelf. The river signal is still very pronounced both in temperature and in salinity profiles, with an efficient mixing over the 60 m layer on the shelf and more concentrated isopycnals over the shelf edge. The most eastern section 7 was conducted under the ice. The temperatures are, thus, negative above the Atlantic Water, but salinity profile reveals the river water presence with the freshwater core having salinity below 29. The maximum value of Brünt-Väisälä frequency are less than for other sections and are observed at 20 m depth and at 55 m depth, following 1024 kg/m^3 and 1026.5 kg/m^3 isopycnals, accordingly, showing the maximum stability of water vertical stratification under the ice.

To summarize, during the summer 2018, we observe a north-eastern displacement of the Lena River water including in the MIZ and ice-covered area. We suggest that the active displacement started in the ice-covered conditions after the maximum of river discharge in June-July (following the **?** study and the Lena River discharge measurements presented in Fig.3), then, with progressive opening, ~~a~~ part of the river water was mixed within the upper sea layer and exchanged heat with the atmosphere. ~~Regarding~~ For the water under the ice, the heat flux from the river water to the sea ice resulted in cooling of ~~these~~ this water to the ambient negative temperature, but, at the same time, the sea ice protected the freshwater layer from wind-induced mixing, so it conserved a pronounced salinity signal.

3.3.4 Tracing surface water origin using oxygen isotopes (delta-O18)

The oxygen isotopes are considered as a "natural tracer of river runoff in the Arctic Ocean" (**?**) and are widely used to detect the origin of water masses (**?**, **?**, **?**). The ~~most simple~~ simplest approach to detect a river water fraction in a water sample is to

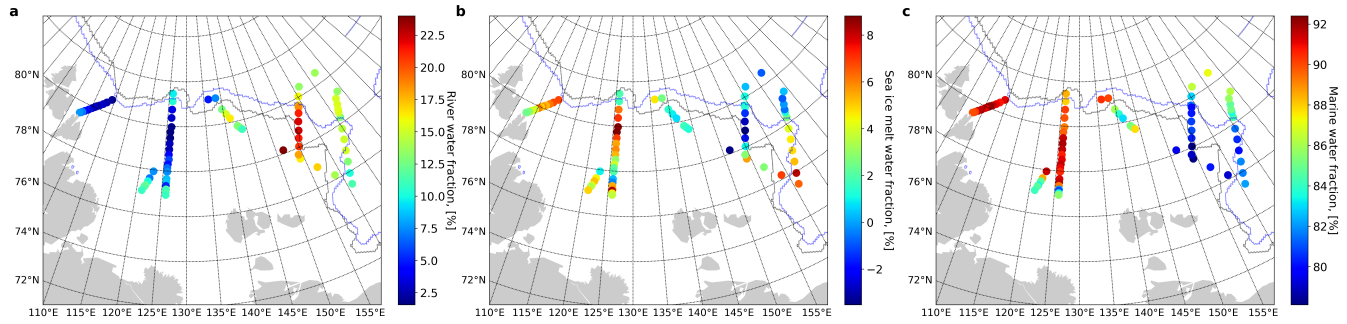

Figure 14. Fractions of river water (a), sea ice melt water (b) and marine water (c), calculated using d-O18 measurements and **?** 3-components model of freshwater balance. A thin black line shows the position of sea ice edge on August 31, 2018, when the northern stations of the meridional (5) section along 126°E were done in the MIZ, and the blue line shows the sea ice edge on September 16, 2020, when the ARKTIKA-2018 expedition was working in the MIZ of the East-Siberian Sea. Please, note that the ~~colorbar~~ colourbar scale is different for each water fraction.

compute a ratio between the measured salinity and oxygen isotope 18 (delta-O18). As ~~it was~~ is described in Data and Methods Section, we used only the surface measurements in the upper ~~3 m~~ 3-m layer.

Using a rather simple three-component model to distinguish the marine water, the river water (meteoric water), and the sea ice melt water described in **?**, we calculated the fractions of each water mass (Fig. 14). In the work of **?**, authors provide values of end-members of this model (typical salinity for each water mass and typical d-O18 concentrations), so after resolving a simple system of three linear equations using the values of the total (measured) salinity and the measured d-O18 concentration, we found a contribution of each fraction. As done in **?**, the role of precipitation is neglected in this model, as its amount is insignificant compared to the river water input. The sea ice melt fraction can be negative in case of sea ice formation.

This analysis indicates that the most important fraction of river water is brought over the shelf and the shelf edge of the East-Siberian Sea (Fig.14, a). At the same time, the water samples at the northern part of the 126°E section consist of 10-15 % of the river water and only of 0-5% of the sea ice melt fraction. Knowing that the main maximum of the river discharge occurs in June (Fig.3), this fact supports our hypothesis that a noticeable amount of river water was distributed under the ice far northward into the deep part of the Laptev Sea (north of 80.5°N), where it will enter the central Arctic Basin later.

It is interesting that the areas with the highest sea ice melt fraction (Fig.14, c) (5-10%) very slowly follow the sea edge, so they were observed in the central and western part of the Laptev sea and in the MIZ area in the East-Siberian Sea. The sea ice formation (the negative values of sea ice melt fraction) is found in MIZ and its vicinity at 78-70°N - ~~150-150~~150-160°E of the East-Siberian Sea, which is expected as these measurements were done in the second part of September 2018, the beginning of freezing season. The presence of river waters may accelerate the sea ice formation if the air temperature favours it.

The surface water samples of the western and central parts of the Laptev sea consist of large marine water fraction (90-95%). The lowest marine water fraction (75-80%) was found over a very shallow ice-free area between the New-Siberian islands and MIZ in the East-Siberian Sea, where both sea ice melt and river water fractions are relatively high (5-10% and 10-25%

respectively). Actually, it is the area of the most intense surface mixing that was observed using ~~in situ~~ *in situ* measurements during the ARKTIKA-2018 expedition.

3.4 Wind forcing.

A previous study in this region (**?**) claimed that the surface fronts displacement is mainly governed by the wind and atmospheric pressure centers. To investigate the role of the wind forcing at the synoptic scales, we compute mean monthly Ekman transport for August and September 2018 (Fig. 15). The calculation is described in the section 2.

The discussed displacement of the river plume extension in August and September ~~are~~ is well seen in both SST and SSS mean monthly fields (Fig.15 a, d and b, e, respectively). The most pronounced feature in the SST field is the drop of SST by 3°C in the central and southern ~~part of the~~ Laptev Sea. ~~The salinification~~ Salinification of the northern, central, and southwestern part is observed in August-September SSS fields. The average wind speeds are low to moderate during August and September, 3-7 m/s (Fig.15 c, f). The wind field in August is more homogeneous and velocities are slightly higher with an overall south-easterly direction; the Ekman transport pushes the river water out of the central part of the Laptev Sea favouring its propagation under the ice. ~~A large area of convergence and downwelling is seen east of the Taimyr peninsula at 77N 120E. Almost the rest of the studied area is an upwelling zone, with large vertical velocity in the Vilkitskiy Strait and following the river front above the continental slope in the central part of the Laptev Sea.~~

In September, the wind changes its main direction to south-westerly, which leads to ~~a river water blocking~~ river water trapped in the Yanskiy bay, still favouring the freshwater flux propagation under the ice, but mostly into the southern part of the East-Siberian Sea. ~~A large-scale divergence and upwelling in the north-west Laptev Sea was observed as well. The Ekman vertical velocities in September differ from August. Several downwelling zones are observed: in front of the Lena delta, close to MIZ in the north-east, and in the deep part of the central Laptev Sea. The irregular pattern of the upwelling and downwelling facilitate the mixing of different water masses, which is more active, thus, in September.~~ As it was shown in the work of **?**, the onshore Ekman transport will generate a coastal downwelling followed by an increase of the salinity over the far-field areas of the river plume and its further offshore entrainment.

4 Discussion and conclusion

Based on ~~in situ~~ *in situ* and satellite measurements, we document the evolution of ~~the~~ water masses during August and September in the Laptev and the East-Siberian Seas. Satellite DMI SST and SMOS SSS "A" estimates are cross-validated with CTD data and continuous TSG measurements ~~and CTD data (~~rarely done in this region~~)~~. For the first time, ~~we follow how the river water input is distributed and where it is stored in the Laptev and the East-Siberian Sea at synoptic scale. It became possible thanks to~~ thanks to the new satellite-derived salinity field (SMOS SSS "A"), a vast range of ~~in situ measurements and also~~ *in situ* measurements and results of geochemical analysis, we follow how the river water input is distributed and where it is stored in the Laptev and the East-Siberian Seas at a synoptic scale.

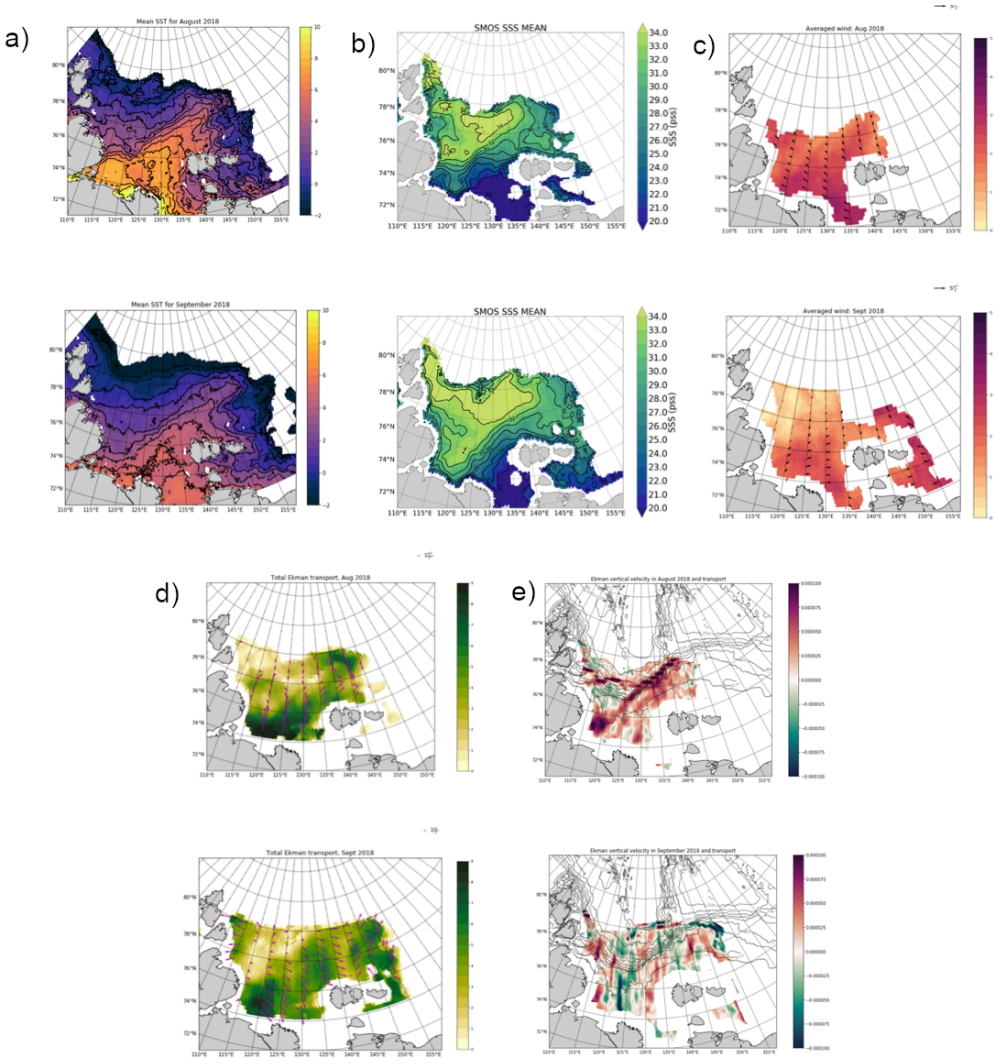

Figure 15. ~~Mean monthly averages for~~ August (~~upper row~~left column) and September (~~lower row~~right column) monthly means of: (a, d) SST, (b, e) SSS, (c, f) wind speed and direction shown with ~~red~~ blue arrows, horizontal Ekman transport is shown with black arrows, total horizontal Ekman ~~vertical velocity (in cm/s)~~ transport is shown with ~~color~~colour

To investigate local surface water masses, we use a variation of a classical TS analysis ~~is studied using~~ from satellite measurements. It ~~helped~~ helps to define new surface water masses adapted for the Eastern Arctic Ocean with a typically low salinity and discuss their transformation. As the validity of SMOS SSS was ~~demonstrated successfully and~~ successfully demonstrated and as SMOS measurements are accessible from 2010 to the present, this technique could be applied for ~~the~~ future studies of the surface water transformation ~~at~~ on different time scales.

The transformation of fresh ~~river water input~~ water mass from river inflow occurs very quickly during the Arctic summer, ~~of the order of~~ over a period of typically 1-2 weeks. ~~Our observationssuggest that the~~ Based on our observations, we suggest that wind-induced vertical mixing, a weaker river discharge, and a continuously decreasing radiative income impact the variability of surface water characteristics, as ~~is particularly well seen in~~ it is well observed at the beginning of September ~~. The second~~ 2018.

Following the classification of coastal buoyancy flows described in **?**, the displacement of river waters over the Laptev Sea shelf can be regarded as a slope-controlled buoyant gravity current, where the buoyancy forces are acting on the water body together with the wind stress and the bottom friction over a large area of the slightly inclined shelf, and at some moment the buoyancy flow detaches from the bottom at a distance W_a. If we suppose that the equilibrium water depth h_p, where the bottom friction becomes 0, is 25 m (based on section 5 southern CTD measurements), in the Laptev Sea it is situated at a distance W_a of 100 km from the Lena River delta, approximately at 75°N, 130°E. The upwelling-favourable winds will induce the offshore Ekman transport and stretch the buoyancy plume over the shelf, while the "downwelling" (onshore) winds will cause a deepening of the isopycnals. A sequence of upwelling-downwelling events can cause a further entrainment and a possible detachment of the buoyant coastal plume to the northern part of the shelf, the continental slope and the deepen part of the Laptev Sea or over the East-Siberian Sea shelf.

The variability in freshwater and the energy sources therefore partly explains the seasonal variability of the buoyant plume. The first yearly maximum of river discharge occurs in ~~the~~ May, after an opening of the sea ice. The second one occurs in the beginning of August. ~~The~~ This warm and fresh river water is redistributed and transformed in the surface layer of the Laptev Sea during the month of August~~, but after~~ . After the passage of several cyclones in the beginning of September, there is no additional ~~important~~ source of heat and fresh water that would maintain the variability of water masses. ~~Globally~~Overall, in September, the ~~water mass CS~~ "cold and saline" water mass progressively occupies the ice-free surface of the Laptev ~~sea~~ Sea instead of other (“transformed”) water masses observed there in August. ~~The ice formation starts at~~ Sea ice growth starts in the end of September ~~and~~ whereas sea surface will be ~~covered by November, so it seems that freezing will begin~~ fully covered by sea ice only by November 2018. The autumn freezing begins only after the heat accumulated during the summer season is released to the atmosphere, and the water temperature at the surface drops to the freezing point.

An overview of **?** describes main mechanisms of the river plume mixing and transport at different distances from the estuary area. Our *in situ* and satellite data make it possible to investigate mostly the "far field" area of the river plume, where the balance between the wind stress and the buoyancy is governing the propagation and mixing of the surface fresh water with the "ambient sea". As it was mentioned, the Ekman transport illustrates an important forcing for the freshwater displacement. As the theoretical Ekman depth is controlled mainly by the Coriolis parameter f and by viscosity, assuming that the viscosity is homogeneous in the south of the Laptev and the East-Siberian Seas, the Ekman depth exceeds the depth of some shallowest areas (according to **?** study in the same region the Ekman depth is $D_{Ekm} = 37$ m: see the position of 37-m isobath in the Laptev Sea in Fig.15). Thus, the calculated Ekman transport should be regarded as a theoretical concept illustrating possible mechanisms of horizontal transport and vertical mixing only in the central and northern areas, whereas over the shallower seas, the dynamics will be more constrained by mixing and the direction of the Ekman currents relative to bathymetric contours.

During the first 10 days of August, the upwelling-favorable north winds (mostly anticyclonic atmospheric conditions) stretched the freshwater plume from the south to the central Laptev Sea up to 78°N. In the second part of August, the wind changed its direction to the westward and (downwelling favourable), so that a buoyancy plume of river waters displaced parallel to the coastline to the East-Siberian Sea. An entrainment of the buoyancy plume is evidenced in the CTD-measurements of salinity in the Eastern Laptev Sea and in the East-Siberian Sea (sections 6-8).

The wind situation in August was favorable for the extreme propagation of river water into the north-eastern part of the Laptev Sea followed by a propagation into the East-Siberian Sea in the MIZ and under the sea ice. The propagation of river water under the sea ice is apparent in the western part of the East-Siberian Sea, where two branches with warm and fresh cores have been observed with *in situ* data (section 6). These branches can be understood as a result of previous entrainments of the Lena River water after a sequence of upwelling-downwelling events, pushing and detaching them offshore. After the river water separated from the estuary, it followed the shelf keeping its freshwater core with salinity below 29 up to the East-Siberian Sea.

A pathway of the low salinity Kara water is observed during several days of our study. The Kara water propagates mostly through the Vilkitskiy Strait and partly through the Shokalskiy Strait, but no freshwater is found northward of the Severnaya Zemlya Archipelago. Propagating along the coastline (as a reminiscent of Kelvin wave starting from the Ob' and Yenisey estuary), the low-salinity Kara water enters the Oleneksiy ~~bay~~ Bay where it meets another freshwater flux from the Khatanga and the Lena rivers. The arrival of freshwater via the Vilkitsiy Strait was already studied using ~~in situ~~ *in situ* data by **?** , ~~**?**~~and **?**. However, this is the first time this event has been observed from satellite ~~data which provide a unique~~ salinity data which provides a unique opportunity for a regular monitoring. The freshwater input from the glaciers and icebergs of the Severnaya Zemlya Archipelago should probably also be taken into account, but this is out of the scope of this study, and we ~~assume~~ have assumed the volume of this source of freshwater ~~as~~ to be negligible compared to the volume of the incoming very fresh Kara Sea water.

~~The wind situation in August was favorable for the extreme propagation of river water into the north-eastern part of the Laptev Sea with following penetration into the East-Siberian Sea in MIZ and under the sea ice. The propagation of river water under the sea ice is apparent in the western part of the East-Siberian Sea, where two branches with warm and fresh cores were observed with in situ data.~~

~~The Ekman transport illustrate a possible forcing for the freshwater displacement. As the theoretical Ekman depth is controlled mainly by the Coriolis parameter f (and also by viscosity), in the south of the Laptev and the East-Siberian Seas it exceeds the depth of some shallowest areas (according to **?** study in the same region the Ekman depth is $D_{Ekm} = 37$ m: see the position of 37-m isobath in the Laptev Sea in Fig.15). Thus, the calculated Ekman transport should be regarded as a theoretical concept illustrating possible mechanisms of horizontal transport and vertical mixing in the central and northern areas. A new sea level dataset provided by DTU for the Arctic Ocean and calculated geostrophic currents, discussed in the Appendix, enriches the overview of the surface ocean dynamics during selected summer months.~~

~~On a~~ At a larger scale, ~~this situation can be also~~ the observed spatial variability can also be explained by a positive (in April-October 2018) Arctic Oscillation index ~~favoring~~ favouring the eastward propagation of fresh water, as it was demonstrated

in ~~works of~~ studies by **?**, **?**, and **?**. An important part of the northward propagation to the shelf edge is not explained by the positive AO. Based on the oxygen isotopes results, we claim that a similar propagation of river water far northward happened before the observed period (in June-July), when the Laptev Sea was still covered with ice and the Lena River discharge was the largest (Fig.3). ~~In the north~~ At the northern end of the 126°E section, under the ice, the upper 25-m layer is fresher with a salinity below 33, which supports this hypothesis. There is no evidence that the sea ice melting itself ~~can create~~ created such a considerable layer of freshwater. Our isotopes estimates could be further refined using alkalinity to separate the meteoric water estimated with water isotopic analysis (river input from precipitation).

A study of **?** also supports the influence of river water, as a similar situation was observed in 2011. Unfortunately, the present spatial resolution of satellite-derived SSS and its uncertainty due to the ~~ice proximity~~ proximity of sea ice makes it difficult to separate river water from the freshening associated with ~~the sea ice melting~~sea ice melt. No accurate satellite measurement of sea ice thickness in ~~MIZ exists~~ the MIZ is available at present to the best of our knowledge, ~~so it is complicated~~ hence it is not easy to evaluate the freshwater input due to the sea ice melting on the scale of several months. Nevertheless, the existing satellite data ~~already have~~ have already a great potential for the Arctic studies of fresh water. To improve ~~our~~ this evaluation of the freshwater budget in the Arctic Ocean, we suggest that appropriate numerical models assimilate the estimates of river discharge, new satellite-derived sea surface salinity and wind data. An attempt to analyze the new sea level dataset provided by DTU (Danish Technological University) for the Arctic Ocean (**?**), and calculated geostrophic currents, is discussed in the Appendix and enriches the overview of the surface ocean dynamics during selected summer months. Nevertheless, at present it seems that an additional work on the continuous ADT estimates over the shallow water is needed to use this dataset for the studies of coastal flow variability.

Appendix A: Altimetry and geostrophic currents

~~Two~~ We calculated two monthly fields of absolute dynamic topography (ADT) and geostrophic currents ~~were calculated~~ from sea level anomalies (SLA) Arctic L4 product and mean dynamic topography (MDT) provided by ~~Danish technological~~ the Danish Technological University (Fig. A1, **?**). Sea level anomalies are available as mean monthly values on a grid adapted to polar regions with 0.25°step for latitudes, and 0.5°step for longitudes. Mean dynamic topography global ~~one-minute model~~ model with one-minute spatial resolution was used to compute ADT. The resulting monthly absolute dynamic topography ($ADT = MDT + SLA$) was calculated for selected summer months.

Overall, the ADT remarkably follows the ocean bottom topography with higher SLA over the shelf and lower SLA over the deep part of the studied area, which corresponds to the study of **?**. The only exception is negative SLA in the Olenekskiy ~~bay~~ Bay in August 2018. We suggest that the general northward wind-induced displacement of the water over the very shallow southern part of the sea was compensated only by the river water inflow to the east of 122°E, close to the Lena River delta. Positive SLA were more pronounced in September than in August, though in August the SST was higher over the southern and central ~~part~~ parts of the Laptev Sea, and the salinity was lower in the Olenekskiy ~~bay~~Bay. The importance of ~~sterical~~ the steric component in variation of the sea level in August-September is thus doubtful, though several ~~source~~ sources of uncertainty can

impact the quality of ~~provided~~ these SLA data: ~~uncertainty in~~ uncertainties in the tidal model, the bathymetry precision, the accuracy of the MDT over the shallow part of the Laptev Sea, etc, as **?** noticed in ~~his~~ their work. It should be noted that SSH variability of the Laptev and the East-Siberian Seas presented in the work of **?** ~~,~~ had the lowest correlation with ~~in situ~~ *in situ* gauge measurements in the Arctic Ocean, because of the "seasonal runoff".

The geostrophic currents were calculated following~~classical formula~~: $u_g = \frac{-g}{f}\frac{dh}{dy}$, $v_g = \frac{g}{f}\frac{dh}{dx}$, where h is ADT, x and y are the distance in metres. Geostrophic currents presented in Fig.A1 are very weak and demonstrate rather chaotic structures during ~~selected months .~~ the summer months of 2018. Among the well-pronounced features, we find an outflow from the Laptev Sea in the Vilkitskiy Strait~~is noticeable~~. Above the continental slope edge, the principal direction of currents is westward with a maximum current speed of 0.5 m/s. ~~In the~~ Further south, an outflow at 122 °E and 130°E contributes to transport the Lena River Water into the central part of the Laptev Sea. In the Yanskiy ~~bay~~ Bay a vortex-like system exists in both August and September 2018. Geostrophic currents in the East-Siberian Sea were calculated from the altimetric measurements in MIZ, so should be interpreted with care. **?** stated that the SSH measurements there cannot reflect the mesoscale phenomena, because of the small Rossby radius (of order 1 km) and the altimeter along-track resolution of 300 m. At the same time, the same study reported the largest eddy kinetic energy in the shallowest areas.

From our calculations, a cyclonic feature of 150 km in diameter is seen at 79°N, 157°E, and might be topographically induced, as well as a similar cyclonic feature at 78.5°N 135°E. An extended study should be carried out to validate the accuracy of altimetry-derived currents in this region with mooring or vessel mounted ADCP measurements.

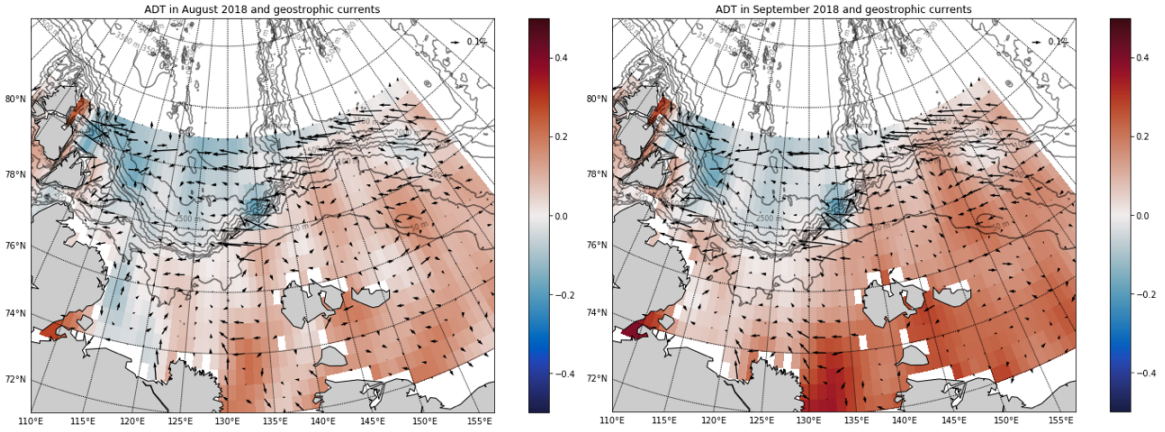

Figure A1. Absolute dynamic topography ~~,~~ (cm) and geostrophic currents ~~,~~ (cm/s~~,~~) in August and September 2018, calculated from DTU monthly Sea Level anomaly

Competing interests. No competing interests are present

Acknowledgements. We thank Jean-Luc Vergely for fruitful discussions about SMOS SSS data filtering in the Arctic ocean. We thank Mattew Alkire, Andrey Novikhin, Natalia Vyazigina, all hydrochemistry team of the ARKTIKA-2018 expedition and Ekaterina Chernyavskaya for the collection of water samples for the oxygen isotopes analysis, their analysis and further discussion. We thank all the scientific team of the ARKTIKA-2018 expedition and the crew of RV Akademic Tryoshnikov for their work. This study was supported by the French CNES-TOSCA SMOS-OCEAN project. Anastasiia Tarasenko, Vladimir Ivanov and Nikita Kusse-Tiuz acknowledge financial support from the Ministry of Science and Higher Education of the Russian Federation, project RFMEFI61617X0076.